Uguna, Jacob Onyebuolise and Carr, Andrew D. and Marshall, Chris and Large, David J. and Meredith, Will and Jochmann, Malte and Snape, Colin E. and Vane, Christopher H. and Jensen, Maria A. and Olaussen, Snorre (2017) Improving spatial predictability of petroleum resources within the Central Tertiary Basin, Spitsbergen: a geochemical and petrographic study of coals from the eastern and western coalfields. International Journal of Coal Geology, 179 . pp. 278-294. ISSN 1872-7840

Improving spatial predictability of petroleum resources within the Central Tertiary Basin, Spitsbergen: A geochemical and petrographic study of coals from the eastern and western coalfields

Jacob O. Uguna[a,*], Andrew D. Carr[c], Chris Marshall[b], David J. Large[b], Will Meredith[a], Malte Jochmann[d,f], Colin E. Snape[a], Christopher H. Vane[e], Maria A. Jensen[f] and Snorre Olaussen[f]

[a] The University of Nottingham, Department of Chemical and Environmental Engineering, Innovation Park, Energy Technologies Building, Jubilee Campus, Nottingham, NG8 1BB, UK

[b] The University of Nottingham, Department of Chemical and Environmental Engineering, University Park, Nottingham, NG7 2RD, UK

[c] Advanced Geochemical Systems Ltd, 1 Towles Fields, Burton on the Wolds, Loughborough, LE12 5TD, UK

[d] Store Norske Spitsbergen Kulkompani AS, P.O. Box 613, N-9171 Longyearbyen, Norway

[e] Centre for Environmental Geochemistry, British Geological Survey, Keyworth, Nottingham, NG12 5GG, UK

[f] The University Centre in Svalbard, P.O. Box 156, N-9171 Longyearbyen, Norway

*Corresponding author: jacob.uguna@nottingham.ac.uk; jay.uguna@gmail.com

Abstract

Central Tertiary Basin (CTB) coals from a variety of palaeogeographic conditions within the Longyear and Verkhnij seams, were sampled to assess the relationship between the petroleum present, the remaining generation potential and coal geochemistry in order to improve the spatial predictability of petroleum resources within the basin. Vitrinite reflectance (VR) values from the CTB coals have been shown to be suppressed (Marshall et al., 2015a). This study attempts to quantify and correct for this suppression effect by applying the Lo (1993) method (LoVR), which uses Hydrogen Index (HI) values to modify VR data, and the coal Rank(S_r) scale of Suggate (2000, 2002), a technique not affected by suppression. In addition, the oil generation and expulsion thresholds for the CTB coals were investigated.

A pseudo-van Krevelen diagram shows that the majority of the coals plot on the Type II kerogen line, while the remainder plot between the Types II and III kerogen lines, with HI between 151 - 410 mg HC/g TOC; however, maceral analysis shows that Type III kerogen predominates. This is attributed to the presence of abundant fluorescing (oil-prone) vitrinites. The LoVR, T_{max} and Rank(S_r) parameters all show that maturity increases from basin margins towards basin centre (i.e. from Bassen to Lunckefjellet, to Breinosa and Colesdalen) and indicate that all the coals are within the oil generation window. The marginal samples at Bassen are within the early mature stage of the oil window (i.e. ~0.7% R_O); meaning the threshold for oil generation in the basin could not be clearly defined. However, the observed maturation trend somewhat parallels the maturation pathway of the New Zealand Coal Band (NZ Coal Band) and the "envelope" of the Sykes and Snowdon (2002) NZ coal data-set; therefore, it is considered that the oil generation threshold for the CTB coals is likely at Rank(S_r) ~9 – 10, T_{max} ~420 – 430 °C in line with the observed rise in Bitumen Index (BI). Some of the Lunckefjellet coals and all the Breinosa and Colesdalen coals have either reached or progressed beyond the threshold for oil expulsion as indicated by the peak in HI at Rank(S_r) ~11 – 12, LoVR ~0.75 – 0.85% R_O, T_{max} ~430 – 440 °C. The peak in BI at Rank(S_r) ~12.5 – 13.5 suggests that some of the Lunckefjellet and Breinosa coals, and all the Colesdalen coals have reached the "effective oil window".

Total sulphur (S_T) contents range between 0.46 – 12.05 % indicating non-marine to strong marine influence upon precursor peats, with S_T contents of the Longyear seam appearing to record instances of coastal retreat associated with base level rise. Marine deposition seems to significantly control the distribution of oil-prone coals within seams and across the CTB. The levels of marine influence (as indicated by S_T content) show clear positive relationships between BI and HI within the Bassen samples because they have not started expelling oil. Conversely, the levels of marine influence show clear negative relationships with BI and HI within the Colesdalen samples because they have commenced oil expulsion, and probably reached the "effective oil window". The more marine influenced coals appear to have commenced petroleum generation relatively earlier, which is a plausible explanation why the coals from the Lunckefjellet locality appear to be at different stages within the oil window.

Keywords

Oil-Prone Coal; Perhydrous Vitrinite; Maturity; VR; LoVR; T_{max}; Rank(S_r); Suppression; Generation; Expulsion; Todalen Member; Spitsbergen.

1. Introduction

The Central Tertiary Basin (CTB) Spitsbergen, Svalbard, contains large reserves of perhydrous (oil-prone) coals, with oil potential attributed to perhydrous vitrinites formed as a consequence of peat deposition under marine influence (Orheim et al., 2007; Marshall et al., 2015a, b). The greatest oil potential in these coals has been hypothesised to be favoured by environmental conditions within the precursor peat including: relatively high marine influence upon the peatlands which resulted in increased sulphur content (≥0.5 %), high bacterial degradation (>100 µg/g TOC hopanes), stable hydrology and fen (rheotrophic) depositional conditions (Marshall et al. 2015a). However, this interpretation is based on samples from only 3 localities in the eastern coalfield, and thus covers only a limited range of palaeogeographic settings, an important factor on the level of marine influence upon the mires in which the CTB peats/coals formed (Marshall et al., 2015a). One of the aims of this study is to re-evaluate the interpretations of Marshall et al. (2015a) using a wider range of samples from multiple seams across 7 localities including the eastern and western coalfields. By doing this, we will re-assess the main control(s) on the petroleum potential of the coals taking into account a wider range of parameters, and so provide a practical guide that could be used in identifying areas of greatest remaining oil potential in the basin.

Source rock maturity can be determined using either vitrinite reflectance (VR), T_{max}, biomarkers etc., although for coals, VR is the most widely used. Reason being that it is the only single parameter that can be measured in coal over a wide range of thermal maturities; i.e. from early maturity (lignite) to post-maturity (low volatile bituminous), and shows relative uniform physio-chemical changes which result in an almost linear increase with increasing thermal stress (Teichmüller and Teichmüller, 1979; Mukhopadhyay, 1994). However, there is a specific problem with perhydrous vitrinites in that they frequently show lower reflectance than the orthohydrous vitrinites, and are often referred to as having suppressed reflectance. The presence, recognition and properties of suppressed VR have been widely discussed (Hutton and Cook, 1980; Taylor and Liu, 1987; Teichmüller, 1989; Raymond and Murchison, 1991; Taylor, 1991; Hao and Chen, 1992; Wilkins et al., 1992; Powell and Boreham, 1994; Petersen and Rosenberg, 1998; Petersen and Vosgerau, 1999; Carr, 2000; Petersen et al., 2009). Marshall et al. (2015b) investigated the unusual VR variations within the CTB coals and concluded that the VR

values are suppressed; these workers observed a general decrease in VR towards the top of the Longyear seam, and roughly estimated the true, non-suppressed VR by adopting the measured VR of the least supressed sample (from the lower parts of the seam) per location sampled. This paper will use two different approaches towards estimating the true maturities of the CTB coals; namely: 1) the Lo (1993) method, which incorporates the HI and measured VR data, and 2) the coal Rank(S_r) scale of Suggate (2000, 2002) which utilises cross plots of calorific value (CV) and volatile matter (VM).

Despite VR being suppressed towards the seam roof, a coal seam can be considered to be isometamorphic. Meaning that the least suppressed values from the lower parts of the seam as reported by Marshall et al. (2015b) are correctly considered as indicators of thermal maturity; however, this study will examine this in detail. Also, the relationship between the data from various maturity parameters will be examined and discussed. If the LoVR values show consistency with other maturity parameters, then the Lo (1993) method may be applied to correct for VR suppression in the absence of the more accurate Suggate (2000, 2002) Rank(S_r) scale or FAMM (fluorescence alteration of multiple macerals) measurement from which the unsuppressed VR can be estimated (Wilkins et al., 1992; 1998; Petersen et al., 2009). In addition to the suppression of VR, T_{max} can also be suppressed in perhydrous coals and source rocks. In a study of New Zealand Eocene coals, Newman et al. (1997) observed that T_{max} was lower in perhydrous coals than in the other coals (orthohydrous) with the same burial and thermal histories. Similarly, the T_{max} values of Canadian Cretaceous high HI coals have been noted to be anomalously low (Snowdon, 1995). Sykes and Snowdon (2002) also observed T_{max} suppression in Late Cretaceous - Cenozoic coals from New Zealand. Therefore, this study will also assess T_{max} suppression within the CTB coals.

Furthermore, this study aims to examine and discuss the thresholds for oil generation and expulsion in the CTB with reference to the maturation pathway(s) defined by published coal data-sets from around the world.

2. Geological setting

The Svalbard archipelago, located between latitude 74° and 81° north, and between longitude 10° and 35° east, is the exposed part of the Barents Sea platform; it is situated on the NW corner of the Eurasian continental plate, with rocks ranging from the Archean to Quaternary in age (Harland et al., 1997). The opening of the North Atlantic Ocean caused dextral movement between Svalbard and eastern Greenland, with oblique compression (transpression) leading to the development of the West

Spitsbergen Fold and Thrust Belt (Eldholm et al., 1987; Bergh et al., 1997; Leever et al., 2011). The transpressional event was probably short lived, being linked to a shift in the spreading direction of the Labrador Sea prior to the earliest Eocene seafloor spreading (Gaina et al., 2009), and there is a suggestion that compression peaked in Early Eocene (Tegner et al., 2011). The CTB and the linked West Spitsbergen Fold and Thrust Belt form a 100 - 200 km wide NNW-SSE striking zone in western and central Spitsbergen, with the wedge-top CTB located in a broad NNW-SSE trending syncline. This structure has a steeper limb to the west and a gently rising limb towards the east (Bergh et al., 1997; Braathen et al., 1999). The basin formed firstly as a broad platform linked to North-East Greenland (Piepjohn et al., 2013) and gradually evolved to a foreland basin, which developed in response to the West Spitsbergen Fold and Thrust Belt (Bruhn and Steel, 2003). The Paleocene - Eocene CTB fill overlies Lower Cretaceous strata and contains the majority of the economic coal bearing units, which belong to the earliest phase of the basin fill deposited in a paralic setting (e.g. Nagy, 2005) within a humid temperate climate (Marshall et al., 2015a). In the CTB, mining is concentrated within the Todalen Mb. of the Firkanten Fm. (Orheim et al., 2007), which is generally dated as early Paleocene (e.g. Livshits, 1974; Harland et al., 1997; Nagy, 2005). Five main coal seams are commonly cited within the Todalen Mb. which are: Svea, Todalen, Longyear, Svarteper and Askeladden seams (Fig. 1). However, in the western parts of the CTB, only three coal seams are present (Nidzny, Verkhnij and Sputnik seams e.g. Marshall, 2013) and there is no report on their oil potential. This study focuses on the Longyear and Verkhnij coals.

3. Samples and methods

3.1. Samples

47 coal samples from the Longyear seam in Bassen, Lunckefjellet and Breinosa (eastern coalfield of the CTB), and the Verkhnij seam in Colesdalen (western coalfield of the CTB) have been used for this study (Fig. 2; Table 1). All 47 samples were previously studied by Marshall et al. (2015b). The samples include outcrops (Bassen) and drill cores (Lunckefjellet, Breinosa and Colesdalen) provided by Store Norske Spitsbergen Kulkompani AS (Store Norske AS). Sampling was done at ~0.04 to 0.30 m intervals (excluding ash layers); given the mismatch between the samples sizes received and the samples sizes required for the different analytical techniques, the rifling, cone and quartering

method was adopted to generate the different sub-samples required for the different analytical methods used in this study.

3.2 Methods

VR, Rock-Eval HI, OI and T_{max} data are from Marshall et al. (2015b), while the Rock-Eval data (S1, S2, TOC, BI and PI) are published supplementary material to Marshall et al., 2015b. New data comprises: CV, VM, maceral analysis, ash yield, total sulphur (S_T), Soxhlet yield, LoVR and Rank(S_r). All data from Mine 7 are from Marshall et al. (2015a).

VR measurement was undertaken using methods contained in ISO 7404-5:2009 and described in Marshall et al. (2015b). Maceral analysis was in accordance with ISO 7404-3:2009 using a LEICA DM4500P microscope fitted with oil immersion objectives. A LED 450 nm, with automatic constant colour intensity control, was used for fluorescence. Maceral analysis (500 points counted) data collection was done using the Hilgers Fossil Man system connected to the microscope. The identification and classification of macerals is according to ICCP (1998), Taylor et al. (1998) and Pickel et al. (2017).

Rank(S_r) was estimated from the CV and VM data provided by Store Norske AS, with the values being converted to dry, mineral-matter and sulphur-free (dmmsf) basis according to the following equations of Suggate (2000, 2002): $CV(Btu/lb)_{dmmf} = 100(Btu/lb - 40S_T)/(100 - f_{dmmsf})$; $VM_{dmmsf} = 100(VM - 0.1A - S_T)/(100 - f_{dmmsf})$; the adjustment factor, $f_{dmmsf} = (1.1Ash) + S_T$. Only the samples with ash yield <20 % were selected for Rank(S_r) estimation according to the recommendations by Sykes and Snowdon (2002), and Suggate (2002) as the mineral-matter free basis adjustment is more precise in coals with low ash.

Rock-Eval 6 analysis used was described in Marshall et al. (2015b). The applied Rock-Eval parameters are: S1 = the quantity of already generated hydrocarbons, S2 = the amount of hydrocarbons produced from the cracking of heavy hydrocarbons and from the thermal breakdown of kerogen, T_{max} = the temperature at which S2 reaches maximum, BI = Bitumen Index (S1*100)/TOC, HI = Hydrogen Index (S2*100)/TOC, OI = Oxygen Index [(CO+CO_2)*100]/TOC, PI = Production Index [S1/(S1+S2)], TOC = Total Organic Carbon [pyrolysed carbon (PC) + residual carbon (RC)], and was measured using Rock-Eval pyrolysis.

To determine the quantity of free bitumen plus already generated oil present in the coals, 2 g of milled coal (<100 µm) was Soxhlet extracted using DCM/methanol mixture (93:7 vol/vol) for a period

of 3 to 8 days until a clear solvent mixture was achieved within the thimble chamber of the Soxhlet. Accuracy and data reliability was checked by repeating 6 samples.

Total sulphur (S_T) and iron (Fe) contents were determined using inductively coupled plasma - atomic emission spectrometry (ICP-AES). Milled samples were initially oven dried overnight at 60 °C, followed by total digestion of between 0.45 - 0.55 g samples successively in: (I) 30 ml nitric acid – 69 % w/v, (II) mixture of 8 ml hydrochloric acid – 36 % w/v, and 2 ml hydrofluoric acid – 40 % w/v, and (III) 15 ml boric acid – 4 % w/v. Acid digestion was done using a CEM MARS5 sealed vessel microwave digestion system (Laban and Atkins, 1999). Following acid digestion, elemental measurement was done using an ICP-AES Perkin-Elmer Optima 3300DV emission spectrometer. Accuracy and data reliability was checked by duplicating 1 sample, alongside SARM18 coal reference material in every batch of 12 samples.

Hydrogen content was determined using a Thermo-Electron Flash EA 1112 Elemental Analyser. The furnace was heated to 900 °C, and sample introduced alongside oxygen to aid combustion. Helium carried the combustion products at 140 mL/min through to a reducing stage before passing into a Gas Chromatography column for separation. Samples were analysed in duplicates alongside blanks.

Ash yield was determined by firstly drying milled samples at 60 °C, followed by the combustion of 1.0 ± 0.1 g in a Carbolite muffle furnace (heating to 825 ºC in 2 hours, and then hold for 3 hours). To check precision, samples were loaded into the furnace in duplicates alongside 2 coal reference materials (SARM18 and SARM19). Blanks were used to check for errors due to flying ashes (i.e. ashes crossing over between crucibles during combustion). Errors on duplicates were monitored throughout to ensure they are: (a) less than 0.1 % for ash content ≤15 wt %, and (b) less than 0.2 % for ash content ≥15 wt %.

4. Results

4.1. Maturity and petrographic composition

VR values range between 0.54 – 0.68, 0.58 – 0.75, 0.59 – 0.69 and 0.65 – 0.80% R_O in Bassen, Lunckefjellet, Breinosa and Colesdalen respectively (Table 2). It has been noted that the VR of the CTB coals is suppressed due to the enrichment of vitrinites with bitumen and/or hydrogen. This is exemplified by the Lunckefjellet coals appearing to show similar/greater VR values than the Breinosa coals despite

Lunckefjellet being up-dip of Breinosa (Marshall et al., 2015b). An alternative method of Lo (1993), which uses HI to modify the VR values was applied (Fig. 3). It is acknowledged that the Lo (1993) method may not be very precise as it is based on VR and HI trends during pyrolysis, with some assumptions regarding the effect that HI has on VR. If the HI is ≤ 300, then there is no change made to vitrinite reflectance, as the model assumes that no suppression has occurred. Also, there are uncertainties arising from manually estimating the true VR from the Lo (1993) model graph. Although it is recommended to use the original HI (HI_O) (i.e. the HI at an immature stage) when applying the Lo (1993) model, the likely T_{max} suppression in these coals means the HI_O estimations from existing mathematical relationships (e.g. Banerjee et al., 1998) are unrealistic. However, it was thought that using the HI is not a major issue after comparing results with published studies. The LoVR (suppression corrected) values for the samples range between 0.65 – 0.73, 0.68 – 0.85, 0.76 – 0.84 and 0.77 – 0.93% R_O in Bassen, Lunckefjellet, Breinosa and Colesdalen respectively, with mean maturities of 0.69, 0.78, 0.80 and 0.88% R_O at these four locations respectively (Fig. 3, Table 2). In comparison, the mean measured VR values (i.e. data with suppression effect) for these four locations are 0.61, 0.64, 0.64 and 0.76% R_O respectively.

Another method of avoiding the problem of VR suppression (e.g. wrongly predicting the maturity of petroleum generation) is by using the coal Rank(S_r) scale of Suggate (2000, 2002) which utilises cross plots of either CV and VM, or atomic H/C and O/C. The Rank(S_r) data for 28 Lunckefjellet, Breinosa and Colesdalen coals were estimated (Fig. 4; Table 2) using CV and VM data (Table 3). Values range between Rank(S_r) 7.0 – 13.7 in Lunckefjellet, 12.5 – 13.8 in Breinosa and 12.9 – 13.9 in Colesdalen, with values averaging 10.3, 13.2 and 13.4 respectively at these localities. T_{max} values range between 425 – 437, 431 – 439, 439 – 447 and 440 – 445 °C (with average values of 430, 434, 443 and 443 °C) in Bassen, Lunckefjellet, Breinosa and Colesdalen respectively (Table 3). Unlike the VR data, the LoVR, Rank(S_r) and T_{max} data indicate that maturity appears to increase from Bassen through Lunckefjellet to Breinosa and Colesdalen.

Maceral analysis indicates that the investigated coals have high vitrinite content, with collotelinite and collodetrinite dominating (Table 2). Coals from the Longyear seam in Bassen, Lunckefjellet and Breinosa have slightly higher vitrinite contents (87.8 – 96.8, 78.4 – 96.0 and 88.6 – 96.9 vol % mmf respectively) than coals from the Verkhnij seam in Colesdalen (70.3 – 87.0 vol % mmf). However, coals from the Verkhnij seam in Colesdalen have higher inertinite contents (12.4 – 27.2 vol % mmf) than coals from the Longyear seam in Bassen, Lunckefjellet and Breinosa (1.4 – 10.6, 1.2 –

16.3 and 1.8 – 9.5 vol % mmf respectively). Liptinite contents are consistently <8.0 vol % mmf in all samples. Microscopic examination under UV light shows the coals contain abundant fluorescing vitrinites with varying degrees of fluorescence, and the liptinites show the strongest fluorescence as expected (Figs. 5a and 5b). The vitrinites in the Breinosa and Colesdalen coals, show stronger fluorescence than those in the Bassen and Lunckefjellet coals. Micrinite, thought to be a relic of oil generation (Taylor et al., 1998) is observed within the coals (fine-grained, white speckles interspersed on some of the vitrinite particles; Fig. 5a-2). Brightly fluorescing oil expulsions from cracks in collodetrinites and collotelinites were observed (Figs. 5a-3 and 5b-3). The interspersed nature of micrinite on vitrinite, and oil expulsion from cracks in vitrinite are consistent with the observations by Orheim et al. (2007). Pyrite framboids (diameter ~2 - 35 μm) also occur in these coals (Figs. 5b-1 and 5b-2), which indicates oxygen-poor depositional conditions (Wilkin and Barnes, 1997; Wignall et al., 2005), associated with relatively high marine influence on the mires in which the peats (coals) formed.

4.2. Chemical data

HI values for the Bassen, Lunckefjellet, Breinosa and Colesdalen samples are: 151 – 282, 227 – 410, 292 – 351 and 242 – 271 mg HC/g TOC respectively (Table 2). Hydrogen (H) was measured only in the Bassen samples (H between 4.8 – 5.5 % daf; Table 3). The majority (12 out of the 14) of the Bassen coals are orthohydrous (H between 4.9 – 5.7 % daf) while the remaining two are subhydrous (H < 4.9 % daf) (Diessel, 1992; Wilkins and George, 2002) with lowest HI values (151 and 153 mg HC/g TOC). There is a strong correlation (R^2 = 0.80) between H and HI for the Bassen samples, which is consistent with previous studies (e.g. Espitalié et al., 1977; Petersen, 2006). Assuming that the good correlation between HI and H holds for the Lunckefjellet, Breinosa and Colesdalen coals, then the HI values may be used as an approximate indicator of whether coals are subhydrous, orthohydrous or perhydrous. In the Longyear seam in Mine 7 (Breinosa), Marshall et al. (2015a) measured H contents ranging between 5.6 – 6.4 % daf, and reported that the majority of the seam may be termed perhydrous (H > 5.7 % daf), with only the basal 20 cm being orthohydrous (H between 4.9 – 5.7 % daf). In this study, the HI values at other localities are generally greater than at Bassen, and considering the HI measured in the Longyear coals by Marshall et al. (2015a) (296 – 384 mg HC/g TOC) are similar to values seen in many of the coals under study, we have therefore assumed that the samples under study are a mixture of orthohydrous and perhydrous coals.

Soxhlet extracts (Table 3) range between 66.2 – 109.6, 54.5 – 153.0, 50.3 – 79.2 and 42.3 – 143.2 mg/g in Bassen, Lunckefjellet, Breinosa and Colesdalen respectively.

The variable but generally high TOC contents (44.5 – 89.8 %) as expected from coals, and the S2 contents (109 – 368 mg/g) (Table 3) indicate that some of the coals may be oil-prone. The S1 range between 3.9 – 19.9 mg/g, and the coals from Breinosa and Colesdalen generally have higher values (mean S1 = 14.5 and 15.2 mg/g respectively) than those from Bassen and Lunckefjellet (mean S1 = 6.8 and 10.7 mg/g respectively) (Table 3). The variations in the S1 and S2 values are in part the result of the variable inorganic matter contents as reflected in the ash yield (between 0.9 and 33.3 wt %; Table 3).

Total sulphur (S_T) contents range between 0.46 – 12.05 % in all samples investigated with a general trend of increase from Bassen through Lunckefjellet to Breinosa and Colesdalen.

5. Discussion

5.1. Kerogen typing and petroleum potential

On a van Krevelen equivalent diagram using OI vs HI (Fig. 6), the Breinosa coals, the Colesdalen coals and most of the Lunckefjellet coals plot on the Type II kerogen line, while a few Lunckefjellet coals, and all the Bassen coals appear to plot between the Type II and III kerogen lines; this is inconsistent with maceral analysis which shows that the coals are dominated by Type III kerogen. The trend in Fig. 6 therefore reflects the petrographic and fluorescence observations described in previous sections and shown in Figs. 5a and 5b. The majority of the coals are within the maximum range of HI values expected for Cenozoic coals (250 – 370 mg HC/g TOC) (Petersen, 2006), with some coals showing higher values (>370 – 410 mg HC/g TOC). The coals with high HI values are likely enriched in paraffinic hydrocarbons (e.g. Killops et al., 1998; Petersen, 2005), possibly due to the presence of long-chain aliphatics in the structure of Cenozoic coals in general (e.g. Petersen and Nytoft, 2006; Petersen et al., 2009) or as a result of bacterial decomposition of organic material and consequently liberating aliphatics from lignin within the precursor peat (Marshall et al., 2015a). The high HI values observed appear directly associated with the presence of hydrogen-enriched vitrinites present in the coals, rather than liptinites whose contents are low in these coals (<8 vol %). It is however noted that the presence of sub-microscopic liptinites in some fluorescing vitrinites (Fig. 5a-2., 5b-1 and 5b-4)

may be possibly contributing to high HI and overall VR suppression (Hutton and Cook, 1980; George et al., 1994; Hao and Chen, 1992; Petersen and Rosenberg, 1998; Petersen, 2006).

Multiple minor S2 peaks with slightly differing T_{max} values have been observed in the Rock-Eval 6 pyrograms in this study (Fig. 7). Multiple S2 peaks in immature samples are considered to represent drilling contaminants (Peters, 1986), but given the maturity and use of brine as the drilling medium in this study, drilling mud contamination is not a likely cause. According to Peters (1986), the heavy ends of oil typically appear as S2 rather than S1, resulting in anomalously low T_{max} values and in extreme cases, a bimodal S2 peak. Although the T_{max} values are high in this study, the observed multiple S2 peaks are possibly related to the release of heavy, liquid hydrocarbons (C_{25} - C_{40}) volatilized at temperatures higher than normal for S1 (i.e. the S1' of Delvaux et al., 1990).

5.2. Maturity assessment

The maturity range of the coals under study (LoVR 0.65 – 0.93% R_O, Rank(S_r) 7.0 – 13.9; excluding the Bassen coals, T_{max} 425 – 445 °C) indicates that the coals are within the "oil window". The Bassen coals are at the early mature stage (mean values: LoVR = 0.69%R_O, T_{max} = 430 °C), the Lunckefjellet coals are at least at the onset of the middle oil window [mean values: LoVR = 0.78%R_O, T_{max} = 434 °C, Rank(S_r) = 10.3], while the Breinosa and Colesdalen samples are well into the middle oil window [mean values: LoVR = 0.80%R_O, T_{max} = 443 °C, Rank(S_r) = 13.2, and LoVR = 0.88%R_O, T_{max} = 443 °C, Rank(S_r) = 13.4 respectively].

The VR vs T_{max}, and LoVR vs T_{max} plots show "no" and "borderline weak/moderate" correlations (R^2 = 0.28 and 0.51 respectively; Figs. 8a and 8b). The lack of good correlation shown in the VR vs T_{max} graph (Fig. 8a) contrasts with the significantly higher correlation shown in the LoVR vs T_{max} graph (Fig. 8b). Although there are errors associated with the measurement of both the LoVR and T_{max} parameters, the improvement shown in the LoVR vs T_{max} graph may reflect the removal of the suppression effect from the VR values, but suppression might still be affecting some of the T_{max} values (Newman et al., 1992; Snowdon, 1995; Sykes and Snowdon, 2002). The lack of good correlation of VR vs T_{max} and LoVR vs T_{max} (Figs. 8a and 8b) contrasts with the good (R^2 not quantified) non-linear correlation between VR and T_{max} for the reflectance range <0.5 to 3.0% R_O described by Teichmüller and Durand (1983), and by Petersen (2006) who observed a good linear correlation (R^2 = 0.87, n = 487) between these parameters. The large data-set obtained from different countries around the world used in the Petersen (2006) study appears to contain both orthohydrous and perhydrous coals (HI ~0 -

470 mg HC/g TOC), with maturities ranging between <0.5 and >4.0% R_O, and the good linear correlation obtained clearly contrasts with the non-linear relationship of Teichmüller and Durand (1983) for a similar range of maturities as those used by Petersen (2006). Teichmüller and Durand (1983) noted that their VR vs T_{max} plot was composed of three successive zones, indicating a succession of different modes in coal pyrolysis. Between 0.5% R_O (T_{max} ~ 425°C) and 1.5% R_O (T_{max} ~ 475°C), correlation between VR and T_{max} is approximately linear, whereas below and above these values, T_{max} increases faster than VR. The maturities of coals in this study occur within the "linear domain" of Teichmüller and Durand (1983), yet in both studies there are some scattering of values in this linear zone.

Plots of Rank(S_r) vs T_{max}, and Rank(S_r) vs LoVR show "weak" correlations (R^2 = 0.46 and 0.31 respectively; Figs 8c and 8d). Sykes and Snowdon (2002) approximated the relationship between Rank(S_r), T_{max} and VR mainly because T_{max} and VR show non-linear increase with temperature prior to catagenesis. Suggate (2002) showed a clear general relationship between Rank(S_r) and VR, with the former being more accurate over the range from peat to the end of the oil window. Because the maturity of the coals in this study occur within the "oil window" and the "linear domain" of Teichmüller and Durand (1983), the scattering of values and the poor correlations between LoVR, T_{max} and Rank(S_r) is mainly attributed to: 1) measurement inaccuracies, 2) fundamental differences between VR, T_{max} and Rank(S_r) even though these parameters are clearly maturity/rank dependent. T_{max} is a measure of the maximum rate of release of hydrocarbons from the whole coal during pyrolysis, VR is obtained from only the vitrinite group macerals, while Rank(S_r) is based on VM and CV, which will be affected if the coals have been oxidised prior to sampling or in storage. T_{max} suppression is also a factor, albeit to a lesser degree. The range of ash yields (between 0.9 – 33.3 wt %) mean that mineral matter might be possibly changing the T_{max} value due to catalytic reactions between the mineral matter and the macerals (Espitalié, 1986). The mineralogy of the ash yield of the Svalbard coals under study was not analysed, but variable mineralogies produced by the changing depositional conditions particularly within the Longyear seam, as discussed by Marshall et al. (2015a), may be a limiting factor in both the LoVR – T_{max} and Rank(S_r) – T_{max} relationships. However, if there is mineral matter effect, there should be a relationship between T_{max} and ash yield (or between T_{max} and TOC), which is not the case. Therefore, mineral matter does not play a significant role. There is the effect that multiple S2 peaks have on the T_{max} which could also be affecting the LoVR – T_{max} and Rank(S_r) – T_{max} correlations.

5.3. The relationships between petroleum present, remaining generation potential and maturity

Petersen (2006) described oil generation from humic coals as a complex, three-phase process involving: (i) onset of petroleum generation, (ii) petroleum build-up in the coal, and (iii) initial oil expulsion, followed by efficient oil expulsion (corresponding to the effective oil window). The HI of immature samples is an indication of the hydrocarbon phase that a source rock may generate as it is buried. The HI_{max} concept which is defined by the HI_{max} line at VR ~0.6 – 1.0% R_O, T_{max} ~430 – 455 °C (Petersen, 2006), or Rank(S_r) ~11 – 12, T_{max} ~430 – 440 (Sykes and Snowdon, 2002), is the increase in HI at the start of petroleum generation up to a maximum (i.e. stages i and ii of petroleum generation) prior to the onset of oil expulsion. In a LoVR vs HI diagram (Fig. 9a), while the Bassen coals plot to the left of the HI_{max} line (stage i of petroleum generation), some of the Lunckefjellet coals plot on the HI_{max} line (stage ii of petroleum generation). However, the majority of the Lunckefjellet coals, and all the Breinosa and Colesdalen coals plot to the right of the HI_{max} line (stage iii of petroleum generation) in Fig. 9a. On the Rank(S_r) vs HI and T_{max} vs HI diagrams (Fig. 9b and 9c respectively), the coals show similarities with the LoVR vs HI diagram as all the Bassen coals and some Lunckefjellet coals are within the stage i generation, some of the Lunckefjellet coals are within stage ii generation, while the remaining coals (i.e. some Lunckefjellet and all the Breinosa and Colesdalen coals) are within stage iii generation. Notably, the HI of the CTB coals do not appear to peak at similar maturity as the world-wide coal data-set of Petersen (2006), with the HI_{max} shifting to higher maturity (0.75 - 0.85% R_O) (Fig. 9a). Conversely, the HI_{max} of the Svalbard coals is a close fit to that of the NZ Coal Band and the "envelope" of the Sykes and Snowdon (2002) NZ coal data-set, at Rank(S_r) 11 – 12 (Fig 9b) and T_{max} 430 – 440 °C (Fig. 9c).

On the maturity vs BI plot, the onset of oil generation is indicated by a marked increase in BI, while the peak in BI indicates a change from increasing to decreasing hydrocarbon saturation of the coal pore structure and probably marks the onset of primary gas generation and the "efficient expulsion of oil" (i.e. the effective oil window) (e.g. Sykes and Snowdon, 2002; Petersen, 2006). On the LoVR vs BI diagram (Fig. 10a), only two Colesdalen coals appear to have reached the efficient oil expulsion stage. The T_{max} vs BI diagram (Fig. 10b) shows only one Breinosa coal appear to have reached efficient oil expulsion stage. Conversely, the Rank(S_r) vs BI diagram (Fig. 10c) shows 12 (out of 28) coals (i.e. from Lunckefjellet, Breinosa and Colesdalen) appear to have reached the efficient oil expulsion stage as indicated by the peak in BI at Rank(S_r) ~12.5 – 13.5. This is consistent with observed oil expulsion from some of the coals and in published studies (e.g. Orheim et al., 2007), and thus suggests that there may be a discrepancy in the LoVR - BI and T_{max} - BI plots, most likely due to suppression effect. Indeed, the coal rank variation in this study is small compared to the NZ Coal Band, and the data-sets of Sykes

and Snowdon (2002) and Petersen (2006), making them more suitable to identify changes in the HI or BI vs maturity trend. However, HI seems to increase from Bassen to Lunckefjellet, and then decrease to Breinosa, with further decrease to Colesdalen, while BI increases from Bassen to Lunckefjellet to Breinosa and Colesdalen which is generally consistent with the maturity trend across these localities.

Production index (PI) is <0.10 in all samples (Table 3), which would be expected if the coals were immature (Peters, 1986) but the coals are all within the oil window with some showing evidence of oil generation (micrinite) and oil expulsion. Low PI is consistent with numerous studies showing that coals generally have low S1 and PI values (e.g. Littke et al., 1990; Petersen et al., 2002; Sykes et al., 2014). The presence of mineral matter in pyrolysed coals can influence S1 and S2 values. It has been shown that when mineral matrix (e.g. calcite, illite) is mixed with different kerogens (Types I and III), the S2 yield can be reduced (e.g. Espitalié et al., 1980; Peters, 1986). The S2 reduction is due to the adsorption of heavy pyrolysate components onto clay minerals, which then act as catalysts in the thermal conversion of some compounds to non-volatile char and light materials (S1). Type III kerogen is most prone to this problem because it generates less pyrolysate per gram of OM than Type I or Type II (Peters, 1986). Such a process would mean that there should be an inverse relationship between S1 and S2. However, there is no inverse relationship possibly because: 1) the coals have high TOC contents and have generated much more petroleum than can possibly be adsorbed onto clays and other minerals, and 2) some of the generated petroleum no longer contributed to the S1 as a result of expulsion. Thus, the mineral matter effect may not be significant, although it cannot be ignored especially with the observed variable ash yields. Low PI values could also be due to lack of expulsion.

5.3. Marine influence and the distribution of oil-prone coals within seams across the CTB

Sulphur (S) content in peat is closely related to its depositional environment. Generally, peats accumulating in a freshwater environment will have lower S contents than peats accumulating under marine influence mainly due to the availability of marine sulphates (e.g. Chou, 2012). In a study of marine influence on coaly source rocks of the Eocene Mangahewa Fm. in the Taranaki Basin, Sykes et al. (2014) stated that total sulphur (S_T) values >0.5 % indicate some degree of marine influence. S_T values of 0.5 – 1.5 % and >1.5 % were considered slightly and strongly marine influenced respectively. Hence, coal S_T content should reflect the amount of marine input into the mires in which the peat/coals formed. The Bassen samples show S_T contents between 0.54 – 1.51 % (Table 3), and therefore can be considered slightly marine influenced as per the classification of Sykes et al. (2014). Across

Lunckefjellet, S_T contents range between 0.46 – 9.97 % indicating a transect of non-marine to strong marine influence. Most of the Breinosa and Colesdalen samples experienced strong marine influence with S_T contents between 1.91 – 6.81, and 1.39 – 12.05 % respectively.

Iron (Fe) seems to have a major control on the S chemistry of the Longyear peatlands (Marshall et al., 2015a). Considering atomic weight, the ratio of Fe to S in pyrite is 0.87; thus Fe/S values in excess of 0.87 are required to convert all available S to pyrite. Fe was only measured for 36 (out of the 47) coals under study with the Fe/S ratio (Table 3) averaging 0.77, which is significantly lower than required (0.87) for total conversion to pyrite. In marine influenced locations like Colesdalen, the bulk Fe/S ratio is much lower (0.50). The overall Fe/S data indicates that the amount of available organic S in these coals is higher in more marine influenced coals than in more inland coals. This is consistent with the study of Marshall et al. (2015a) which shows that within the Longyear seam in Mine 7 (Breinosa), there is a shift from Fe-rich (below 80 cm) to S-rich (above 80 cm) sections, which favours oil potential above 80 cm at this location.

S_T content has been found to control the oil potential of coals (e.g. Sykes et al., 2014; Marshal et al., 2015a and references within). Considering only the Lunckefjellet samples in the Rank(S_r) vs BI diagram (Fig. 10c) for example, the high sulphur coals are generally furthest into the oil window and plot in close proximity to each other. Some high sulphur coals appear to have reached the effective oil window, while the low sulphur coal and all the medium sulphur coals have not. The relationship between marine influence and oil generation and expulsion is further investigated by comparing scatter plots of S_T vs BI and S_T vs HI between the least mature (Bassen) and most mature (Colesdalen) samples under study (Fig. 11). At Bassen, the S_T vs BI and S_T vs HI plots show clear positive relationships; conversely, there are negative relationships at Colesdalen. The positive relationships observed at Bassen probably reflects lack of expulsion and low maturity, whilst the negative relationships observed at Colesdalen arises because the coals have commenced expulsion. The more marine influenced samples appear to start generation before the less marine influenced ones, which is consistent with the published effects of sulphur on maturation and petroleum generation in geological basins (Baskin and Peters, 1992; Lewan, 1998). Whilst this observation (i.e. relatively earlier expulsion from the more marine influenced coals) is perhaps due to more favourable conditions for perhydrous coal formation, an outlying high sulphur coal from Lunckefjellet is still at the onset of oil generation (Fig. 10c). This issue may be related to the use of total sulphur (and not organic sulphur) in this study as very high marine influence will

generally result in greater ash yield as shown later in this section and in literature (e.g. George et al., 1994).

The level of marine influence on the Longyear seam in Mine 7 (Breinosa) has been linked with rising sea levels which resulted in greater oil potential in the upper seam, i.e. from ~80 cm to seam top (Marshall et al., 2015a). Within the Longyear seam at Bassen, S_T decreases from ~1.0 % at seam base, to a minimum of ~0.5 % at around 109 cm above seam base, and then increases to ~1.5 % at seam top (Fig. 12a); this trend reflects decreasing sea level from seam base, followed by increasing sea level to the top of seam, which is consistent with the Marshall et al. (2015a) study. At Lunckefjellet BH15-2011 locality, relative increase in sea level from 90 cm towards the top of the Longyear seam was also observed (Fig. 12b), although there is an S_T peak at 80 cm. At Breinosa BH4-2009 locality, the S_T profile from base to top of the Longyear seam (Fig. 12c) also clearly reflects decreasing – increasing sea levels. Within the Verkhnij seam in Colesdalen BH3-2008 locality, a decreasing - increasing sea level trend is not so obvious (Fig. 12d) as in the three localities previously discussed, but the S_T contents of the lower part of the seam (mean value from seam base to 57.5 cm = 1.6 % S_T) is also lower than in the upper part (mean value from 122.5 cm to seam top = 2.9 % S_T), i.e. excluding the outlier (S_T peak at 80.5 cm = 15.9 %). The S_T peak in BH3-2008 (Fig. 12d) possibly resulted from seawater inundation, likely assisted by local topography. The foregoing interestingly shows that sulphur in coal may record instances of coastal retreat associated with base level rise, which is consistent with the study of marine influenced Greta Seam in the Sydney Basin (George et al., 1994). The absence of the decrease – increase in sea levels trend in BH3-2008 is possibly due to greater marine influence associated with closer proximity to the palaeocoastline. This, in addition to the lower vitrinite and higher inertinite contents of the Verkhnij seam compared to the Longyear seam, could also indicate that these two seams are not time equivalent.

In practice, the schematic N-S transect across Adventdalen, i.e. from Bassen to Mine 7 to BH4-2009 (Fig. 13) shows that oil potential on an economic basis (mg/g coal) is dependent upon the balancing of sufficient marine influence to produce and preserve oil-prone materials (as described in Marshall et al., 2015a; Uguna, 2016) with the need for low mineral matter deposition to prevent the dilution of the weakly oil-prone organic carbon within the coals. Towards the coast, high water tables (which favour vitrinite over inertinite formation; e.g. Taylor et al., 1998) are consistent, with greatest sulphur contents and alkalinity; however, the threat of seawater inundation is also greatest in these areas. Inundation results in increasing mineral matter content and limits seam thickness, which

consequently limits oil potential. At the basin margins, marine influence is relatively limited, reducing the ability to produce and preserve oil-prone source materials within the coals. Therefore, an intermediate position within the paralic system appears to have the greatest potential for the production of oil-prone coals.

6. Conclusions

Hydrocarbons present and the remaining generation potential of Spitsbergen coals from Bassen, Lunckefjellet, Breinosa (Longyear seam) and Colesdalen (Verkhnij seam) have been studied by analyses including: maturity, oil potential versus marine influence upon the mires in which the coals formed, and the threshold for oil generation and expulsion. Results show that:

- On a van Krevelen equivalent diagram, the majority of coals plot on the Type II kerogen line, while others plot between the Types II and III kerogen lines, with HI values between 151 - 410 mg HC/g TOC; yet the maceral analysis shows that Type III kerogen predominates. This HI range arises from the presence of fluorescing (oil-prone) vitrinites in the coals, and thus shows that the classical kerogen interpretation lines are not applicable to Cenozoic coals. The PI values are low (<0.10) in all samples, and thus appear to contradict oil generation and expulsion, possibly because: 1) some of the generated petroleum no longer contributed to the S1 as a result of expulsion, and 2) lack of expulsion if part of the generated hydrocarbons is trapped in the coal matrix and not released during thermal vaporisation, but are released during the S2 phase when the kerogen breaks down.

- The VR of the coals are suppressed. Suppression was removed by using the modification based on the HI values of the coals (Lo, 1993); this shows that all samples are within the oil generation window, with mean LoVR values of 0.68, 0.78, 0.80 and 0.88% R_O in Bassen, Lunckefjellet, Breinosa and Colesdalen respectively. The Rank(S_r) scale of Suggate (200, 2002) shows mean values of 10.3, 13.2 and 13.4 in Lunckefjellet, Breinosa and Colesdalen respectively. Both the LoVR and Rank(S_r) values are consistent with the T_{max} values which average 430, 434, 443 and 443 °C at these locations respectively. The correlations between VR, LoVR, T_{max} and Rank(S_r) are poor due to: 1) suppression effect on VR, with lesser suppression effect on T_{max} and LoVR and 2) analytical issues.

- The least mature samples in the CTB data-set are close to the early mature stage of the oil window (i.e. ~0.7% R_O), and thus the threshold for oil generation could not be clearly defined. However, as the maturation trend of the CTB coals closely follows that of the NZ Coal Band and the NZ coal data-set of Sykes and Snowdon (2002), the oil generation threshold for these coals is likely at Rank(S_r) ~8 – 9, T_{max} ~420 – 430 °C as indicated by the rise in BI. Some of the Lunckefjellet coals and all the Breinosa and Colesdalen coals have either reached or progressed beyond the threshold of oil expulsion as indicated by the peak in HI at Rank(S_r) ~11 – 12, LoVR ~0.75 – 0.85% R_O, T_{max} ~430 – 440 °C, while the remainder Lunckefjellet coals and all the Bassen coals are at relatively earlier stages of the oil window. Some of the Lunckefjellet and Breinosa coals, and all the Colesdalen coals appear to have reached the effective oil window as indicated by the peak in BI at Rank(S_r) ~12.5 – 13.5. The observed closeness between the maturation pathways of the CTB coals and the NZ coals emphasises the similarities between the two oil generating systems.

- Oil potential resulted from marine sulphate deposition upon the mires in which the peats/coals formed, and subsequent marine sulphur incorporation during diagenesis. The sulphur contents range between 0.46 – 12.05 % in the coals, and thus indicate non-marine to strong marine influence. The level of marine influence show clear positive relationships between BI and HI within the Bassen samples likely because they are early mature and have not started expelling oil. Conversely, the level of marine influence shows clear negative relationships with BI and HI within the Colesdalen samples because they have commenced expulsion and probably reached the ”effective oil window”. The more marine influenced coals appear to start petroleum generation relatively earlier compared to the less marine influenced ones. Highest hydrocarbon yields are expected in an intermediate position on the coastal plain where marine sulphur is sufficient to preserve oil-prone components, but mineral matter contents are low enough not to dilute TOC. Results indicate that S in coal may record instances of coastal retreat associated with base level rise, which has implications for the stratigraphic interpretations of coals.

Acknowledgements

Sincere appreciation and thanks to Store Norske AS for the financial sponsorship, the provision of samples and support during field work in Svalbard. The University of Nottingham and The University Centre In Svalbard are gratefully acknowledged for the lead author’s studentship opportunities. The

lead author is particularly grateful for been awarded the University of Nottingham's Dean of Engineering Research Scholarship for International Excellence. Special thanks to the Centre for Environmental Geochemistry, British Geological Survey, Nottingham, for Rock-Eval 6 pyrolysis.

References

Banerjee, A., Sinha, A.K., Jain, A.K., Thomas, N.J., Misra, K.N., Chandra, K., 1998. A mathematical representation of Rock-Eval hydrogen index vs T_{max} profiles. Organic Geochemistry 28 (1/2), 43–55.

Baskin, D.K., Peters, K.E., 1992. Early Generation Characteristics of a Sulphur-Rich Monterey Kerogen. AAPG Bulletin 76 (1), 1–13.

Bergh, S.G., Braathen, A., Andresen, A., 1997. Interaction of basement-involved and thin-skinned tectonism in the Tertiary fold-thrust belt of central Spitsbergen, Svalbard. AAPG Bulletin 81(4), 637–661.

Braathen, A., Bælum, K., Christiansen, H.H., Dahl, T., Eiken, O., Elvebakk, H., Hansen, F., Hanssen, T.H., Jochmann, M., Johansen, T.A., Johnsen, H., Larsen, L., Lie, T., Mertes, J., Mørk, A., Mørk, M. B., Nemec, W., Olaussen, S., Oye, V., Rød, K., Titlestad, G.O., Tveranger, J., Vagle, K., 2012. The Longyearbyen CO_2 Lab of Svalbard, Norway - initial assessment of the geological conditions for CO2 sequestration. Norwegian Journal of Geology 92, 353–976.

Brown, H.R., Cook, A.C., Taylor, G.H., 1964. Variations in the properties of vitrinite in isometamorphic coal. Fuel 43, 111–124.

Bruhn, R., Steel, R., 2003. High-resolution sequence stratigraphy of a clastic foredeep succession (Paleocene, Spitsbergen): An example of peripheral-bulge-controlled depositional architecture. Journal of Sedimentary Research 73 (5),745–755.

Carr, A.D., 2000. Suppression and retardation of vitrinite reflectance, part 1. Formation and significance for hydrocarbon generation. Journal of Petroleum Geology 23, 313-34.

584 Chou, C-L., 2012. Sulfur in coals: A review of geochemistry and origins. International Journal of Coal
585 Geology 100, 1–13.
586
587 Delvaux, D., Martin, H., Leplat, P., Paulet, J., 1990. Comparative Rock-Eval pyrolysis as an improved
588 tool for sedimentary organic matter analysis. Organic Geochemistry 16, 1221–1229.
589
590 Eldholm, O., Thiede, J., Taylor, E., 1987. Evolution of the Norwegian continental margin: background
591 and objectives. In Eldholm, O., Thiede, J., Taylor, E., et al., Proc. ODP, Init. Repts., 104: College Station,
592 TX (Ocean Drilling Program), 5–25.
593
594 Espitalié, J., 1986. Use of T_{max} as a maturation index for different types of organic matter. Comparison
595 with vitrinite reflectance. In: Burrus, J. (Ed.), Thermal modelling in sedimentary basins. Paris: Editions
596 Technip. 475–496.
597
598 Espitalié, J., Laporte, J.L., Madec, M., Marquis, F., Leplat, P., Paulet, J., Boutefeu, A., 1977. Methode
599 rapide de caracterisation des roches meres, de leur potential petrolier et de leur degre d'evolution. Rev.
600 Inst. Fr. Per. 32, 23-42.
601
602 Espitalié, J., Madec, M., Tissot, B., 1980. Role of mineral matrix in kerogen pyrolysis: influence on
603 petroleum generation and migration. AAPG Bulletin 4, 59–66.
604
605 Gaina, C., Gernigon, L., Ball, P., 2009. Palaeocene-Recent plate boundaries in the NE Atlantic and the
606 formation of the Jan Mayen microcontinent. Journal of the Geological Society 166, 601-616.
607
608 George, S.C., Smith, J.W., Jardine, D.R., 1994. Vitrinite reflectance suppression in coal due to marine
609 transgression: Case study of the organic geochemistry of the Greta Seam, Sydney Basin. Australian
610 Petroleum Exploration Association Journal 34, 241–255.
611
612 Hao, F., Chen, J., 1992. The cause and mechanism of vitrinite reflectance anomalies. Journal of
613 Petroleum Geology 15, 419–434.
614

615 Harland, W.B., Anderson, L.M., Manasrah, D., Butterfield, N.J., Challinor, A., Doubleday, P.A.,
616 Dowdeswell, E.K., Dowdeswell, J.A., Geddes, I., Kelly, S.R.A., Lesk, E.L., Spencer, A.M. Stephens,
617 C.F., 1997. The Geology of Svalbard. Geological Society Memoir 17, 1–521.
618
619 Helland-Hansen, W., 1990. Sedimentation in a Paleogene foreland basin, Spitsbergen. AAPG Bulletin
620 74, 260–272.
621
622 Hutton, A.C., Cook, A.C., 1980. Influence of alginite on reflectance of vitrinite from Joadja, NSW, and
623 some other coals and oil shales containing alginite. Fuel 59, 711–714.
624
625 International Organisation for Standardisation (ISO) (2009) Methods for the petrographic analysis of
626 coals - Part 3: Method of determining maceral group composition - ISO 7404-3:2009, ISO, Geneva.
627
628 International Organisation for Standardisation (ISO) (2009) Methods for the petrographic analysis of
629 coals - Part 5: Method of determining microscopically the reflectance of vitrinite - ISO 7404-5:2009, ISO,
630 Geneva.
631
632 Jarvie, D.M., Claxton, B.L., Henk, F.B., Breyer, J.T., 2001. Oil and shale gas from the Barnett Shale,
633 Ft. Worth Basin, Texas (Abstracts). AAPG Bulletin 85, 100 pp.
634
635 Killops, S.D., Gunnel, R.H., Suggate, R.P., Sykes, R., Peters, K.E., Walters, C., Woolhouse, A.D.,
636 Weston, R.J., Boudou, J.P., 1998. Predicting generation and expulsion of paraffinic oil from vitrinite rich
637 coals. Organic Geochemistry 29 (1-3), 1–21.
638
639 Laban, K.L., Atkins, B.P., 1999. The determination of minor and trace element associations in coal using
640 a sequential microwave digestion procedure. International Journal of Coal Geology 4 (41), 351–369.
641
642 Leever, K.A., Gabrielsen, R.H., Faleide, J.I., Braathen, A., 2011. A transpressional origin for the West
643 Spitsbergen fold-and-thrust belt: Insight from analog modeling. Tectonics 30 (2), TC2014, DOI:
644 10.1029/2010TC002753.
645

646 Lewan, M.D., 1998. Sulphur-radical control on petroleum formation rates. Nature 391,164–166.
647
648 Littke, R., Leythaeuser, D., Radke, M., Schaefer, R.G., 1990. Petroleum generation and migration in
649 coal seams of the Carboniferous Ruhr Basin, northwest Germany. In: Durand, B., Behar, F. (Eds.),
650 Advances in organic geochemistry 1989, part I, organic geochemistry in petroleum exploration. Organic
651 Geochemistry 16, 247–258.
652
653 Livshits, Y.Y., 1974. Paleogene deposits and the platform structure of Svalbard. Skrifter-Norsk
654 Polarinstitutt 159, 50 pp.
655
656 Lo, H.B., 1993. Correction criteria for the suppression of vitrinite reflectance in hydrogen-rich kerogens:
657 preliminary guidelines. Organic Geochemistry 20 (6), 653–657.
658
659 Marshall, C.J., 2013. Palaeogeographic development and economic potential of the coal-bearing
660 Palaeocene Todalen Member, Spitsbergen. Ph.D. Thesis, University of Nottingham, United Kingdom.
661
662 Marshall, C., Large, D.J., Meredith, W., Snape, C.E., Uguna, C., Spiro, B.F., Orheim, A., Jochmann,
663 M., Mokogwu, I., Wang, Y., Friis, B., 2015a. Geochemistry and petrology of Palaeocene coals from
664 Spitsbergen - Part 1: oil potential and depositional environment. International Journal of Coal Geology
665 143, 22–33.
666
667 Marshall, C., Uguna, J., Large, D.J., Meredith, W., Jochmann, M., Friis, B., Vane C., Spiro, B.F., Snape,
668 C.E., Orheim, A., 2015b. Geochemistry and petrology of Palaeocene coals from Spitzbergen - Part 2:
669 maturity variations and implications for local and regional burial models. International Journal of Coal
670 Geology 143, 1–10.
671
672 Mukhopadhyay, P.K., 1994. Vitrinite reflectance as maturity parameter: petrographic and molecular
673 characterization and its applications to basin modelling. In: Mukhopadhyay, P.K., Dow, W.G. (Eds.),
674 Vitrinite reflectance as a maturity parameter: applications and limitations: American Chemical Society
675 Symposium Series 570, 1–24.
676

677 Müller, R.D., Spielhagen, R.F., 1990. Evolution of the Central Tertiary Basin of Spitsbergen: towards a
678 synthesis of sediment and plate tectonic history. Palaeogeography, Palaeoclimatology, Palaeoecology
679 80 (2), 153–172.
680
681 Nagy, J., 2005. Delta-influenced foraminiferal facies and sequence stratigraphy of Paleocene deposits
682 in Spitsbergen. Palaeogeography Palaeoclimatology Palaeoecology 222, 161–179.
683
684 Newman, J., Price, L.C., Johnston, J.H., 1997. Hydrocarbon source potential and maturation in Eocene
685 New Zealand vitrinite-rich coals: insights from traditional coal analyses, and Rock-Eval and biomarker
686 studies. Journal of Petroleum Geology 20, 137-163.
687
688 Orheim, A., Bieg, G., Brekke, T., Horseide, V., Stenvold, J., 2007. Petrography and geochemical
689 affinities of Spitsbergen Paleocene coals, Norway. International Journal of Coal Geology 70, 116–136.
690
691 Peters, K.E., 1986. Guidelines for evaluating petroleum source rock using programmed pyrolysis.
692 AAPG Bulletin 70 (3), 318–329.
693
694 Petersen, H.I., 2002. A re-consideration of the 'oil window' for humic coal and kerogen type III source
695 rocks. Journal of Petroleum Geology 25, 407–432.
696
697 Petersen, H.I., 2005. Oil generation from coal source rocks: the influence of depositional conditions and
698 stratigraphic age. Geological Survey of Denmark and Greenland, Bulletin 7, 9–12.
699 Petersen, H.I., 2006. The petroleum generation potential and effective oil window of humic coals related
700 to coal composition and age. International Journal of Coal Geology 67 (4), 221–248.
701
702 Petersen, H.I., Andsbjerg, J., Bojesen-Koefoed, J.A., Nytoft, H.P., 2000. Coal-generated oil: source
703 rock evaluation and petroleum geochemistry of the Lulita Oilfield, Danish North Sea. Journal of
704 Petroleum Geology 23, 55–90.
705

706 Petersen, H.I., Bojesen-Koefoed, J.A., Nytoft, H.P., 2002. Source rock evaluation of Middle Jurassic
707 coals, northeast Greenland, by artificial maturation: aspects of petroleum generation from coal. AAPG
708 Bulletin 86, 233–256.
709
710 Petersen, H.I., Nytoft, H.P., 2006. Oil generation capacity of coals as a function of coal age and aliphatic
711 structure. Organic Geochemistry 37, 558–583.
712
713 Petersen, H.I., Rosenberg, P., 1998. Reflectance retardation (suppression) and associated rock
714 properties related to Middle Jurassic coals, Danish North Sea hydrogen-enriched vitrinite. Journal of
715 Petroleum Geology 21, 247–263.
716
717 Petersen, H.I., Sherwood, N., Mathiesen, A., Fyhn, M.B.W., Dau, N.T., Russell, N., Bojesen-Koefoed,
718 J.A., Nielsen, L.H., 2009. Application of integrated vitrinite reflectance and FAMM analyses to solve
719 problems in thermal maturity assessment of the northeastern Malay Basin, offshore SW Vietnam:
720 implications for petroleum prospectivity evaluation. Marine and Petroleum Geology 26, 319–332.
721
722 Petersen, H.I., Vosgerau, H., 1999. Composition and organic maturity of Middle Jurassic coals, North-
723 East Greenland: evidence for liptinite-induced suppression of huminite reflectance. International Journal
724 of Coal Geology 41, 257–274.
725
726 Petersen, T.G., Thomsen, T.B., Olaussen, S., Stemmerik, L., 2016. Provenance shifts in an evolving
727 Eurekan foreland basin; the Tertiary Central Basin, Spitsbergen. Journal Geological Society London
728 173, 634-648.
729
730 Piepjohn, K., von Gosen, W., Läufer, A., McClelland W.C., Estrada, S., 2013. Ellesmerian and Eurekan
731 fault tectonics at the northern margin of Ellesmere Island (Canadian High Arctic) Z. Dt. Ges. Geowiss.
732 German Journal of Geoscience 164, 81–105.
733
734 Pickel, W., Kus, J., Flores, D., Kalaitzidis, S., Christanis, K., Cardott, B.J., Misz-Kennan, M., Rodrigues,
735 S., Hentschel, A., Hamor-Vido, M., Crosdale, P., Wagner, N., ICCP, 2017. Classification of liptinite –
736 ICCP System 1994. International Journal of Coal Geology 169, 40–61.

737

738 Powell, T.G., Boreham, C.J., 1994. Terrestrially sourced oils: where do they exist and what are our
739 limits of knowledge? - A geochemical perspective. In: Scott, A.C., Fleet, A.J. (Eds.), coal and coal-
740 bearing strata as oil-prone source rocks? Geological Society Special Publication 77, 11–29.

741

742 Raymond, A.C., Murchison, D.G., 1991. Influence of exinitic macerals on the reflectance of vitrinite in
743 Carboniferous sediments of the Midland Valley of Scotland. Fuel 70, 155–161.

744

745 Snowdon, L.R., 1995. Rock-Eval T_{max} suppression: documentation and amelioration. AAPG Bulletin 79,
746 1337–1348.

747

748 Suggate, R.P., 2000. The Rank(S_r) scale: its basis and its applicability as a maturity index for all coals.
749 New Zealand Journal of Geology and Geophysics 43, 521–553.

750

751 Suggate, R.P., 2002. Application of Rank(S_r), a maturity index based on chemical analyses of coals.
752 Marine and Petroleum Geology 19, 929–950.

753

754 Sykes, R., Snowdon, L.R., 2002. Guidelines for assessing the petroleum potential of coaly source rocks
755 using Rock-Eval pyrolysis. Organic Geochemistry 33, 1441–1455.

756

757 Sykes, R., Volk, H., George, S.C., Ahmed, M., Higgs, K.E., Johansen, P.E., Snowdon, L.R., 2014.
758 Marine influence helps preserve the oil potential of coaly source rocks: Eocene Mangahewa Formation,
759 Taranaki Basin, New Zealand. Organic Geochemistry 66, 140–163.

760

761 Taylor, G.H., 1991. Reflections on reflectance. Advances in the Study of the Sydney Basin. 25th
762 Newcastle Symposium Proceedings, 222–226.

763

764 Taylor, G.H., Liu, S.Y., 1987. TEM and coal structure. In: Moulin, J.A., Nater, K.A., Chermin, H.A.G.
765 (Eds.), Proceedings, International Conference on Coal Science, Maastricht, 29–32.

766

767 Taylor, G.H., Teichmüller, M., Davis, A., Diessel, C.F.K., Littke, R., Robert, P., 1998. Organic Petrology.
768 Berlin: Gebrüder Borntraeger.
769
770 Teichmüller, M., Teichmüller, R., 1979. Diagenesis of coal (coalification). In: Larson, G., Chilingar, G.V.
771 (Eds.), Diagenesis in sediments and sedimentary rocks. Amsterdam: Elsevier. 207–246.
772
773 Tegner, C., Storey, M., Holm, P.M., Thorarinsson, S.B., Zhao, X., Lo, C.H., Knudsen, M.F., 2011.
774 Magmatism and Eurekan deformation in the High Arctic Large Igneous Province: 40Ar–39Ar age of Kap
775 Washington Group volcanics, North Greenland. Earth and Planetary Science Letters 303(3-4), 203–
776 214.
777
778 Teichmüller, M., 1989. The genesis of coal from the viewpoint of coal petrology. International Journal
779 of Coal Geology 12, 1–87.
780
781 Teichmüller M., Durand B., 1983. Fluorescence microscopical rank studies on liptinites and vitrinite in
782 peat and coals, and comparison with the results of the Rock-Eval pyrolysis. International Journal of
783 Coal Geology 2, 197–230.
784
785 Uguna, J., 2016. Maturity, source rock and retorting potential of the perhydrous coals in the Central
786 Tertiary Basin, Spitsbergen. Ph.D. Thesis, University of Nottingham, United Kingdom.
787
788 Wignall, P.B., Newton, R., Brookfield, M.E., 2005. Pyrite framboid evidence for oxygen-poor deposition
789 during the Permian-Triassic crisis in Kashmir. Palaeogeography Palaeoclimatology Palaeoecology 216,
790 183–188.
791
792 Wilkin, R.T., Barnes, H.L., 1997. Formation processes of framboidal pyrite. Geochim. Cosmochim. Acta
793 61, 323–339.
794
795 Wilkins, R.W.T., Buckingham, C.P., Sherwood, N., Russell, N.J., Faiz, M., Kurusingal, J., 1998. The
796 current status of the FAMM thermal maturity technique for petroleum exploration in Australia, APPEA
797 Journal 38, 421–437.

Wilkins, R.W.T., Wilmshurst, J.R., Russel, N.J., Hladky, G., Ellacott, M.V., Buckingham, C., 1992. Fluorescence alteration and the suppression of vitrinite reflectance. Organic Geochemistry 18 (5), 629–640.

Table captions

Table 1. Coal samples, seams and locations (all samples are part of Marshall et al. 2015b)

Table 2. Maceral composition, VR, LoVR and Rank(S_r) data. Tel = Telinite, Clt = Collotelinite, Cld = Collodetrinite, Vtd = Vitrodetrinite, Cpg = Corpogelinite, F = Fusinite, Sf = Semifusinite, Fg – Funginite, Mac = Macrinite, Mic = Micrinite, In = Inertodetrinite, Sp = Sporinite, Cut = Cutinite, Res = Resinite, Bit = Bituminite, Sb = Suberinite, Lpd = Liptodetrinite. STDEV range for VR and LoVR = 0.03 – 0.09 and 0.03 – 0.05% R_O respectively based on 100 R_O measurements per sample.

Table 3. Chemical data: Rock-Eval pyrolysis, hydrogen (H), Soxhlet yield, total sulphur (S_T), iron (Fe), Fe/S ratio, coal ash, volatile matter (VM) and calorific value (CV). HI in mg HC/g TOC. OI in mg ($CO+CO_2$)/g TOC. BI (Bitumen Index) = (S1*100)/TOC in mg HC/g TOC. H in wt % daf.

Figure captions

(Printed version of figures in black-and-white)

Fig. 1. The van Mijenfjorden Group representing the sedimentary infill of the CTB, Spitsbergen (Adapted from Marshal et al., 2015b). Note: multiple coal seams (S = Svea, T = Todalen, L = Longyear, Vs. = Svarteper, A = Askeladden) occurring within the basal Todalen Mb.

Fig. 2. Map of the northern Central Tertiary Basin in Spitsbergen showing sampling localities and sample types (modified from http://toposvalbard.npolar.no/).

Fig. 3. Model for correcting VR suppression (modified from Fig. 1 of Lo, 1993). Note: the estimated true VR (R_T) in Bassen, Lunckefjellet, Breinosa and Colesdalen are 0.68, 0.78, 0.80 and 0.88% R_O

828 respectively. STDEV of Lo (1993) corrected VR are 0.02, 0.04, 0.05 and 0.05% R_O respectively in all
829 four areas.
830
831 **Fig. 4.** Determination of the Rank(S_r) of the CTB coals using CV and VM (after Suggate, 2002).
832
833 **Fig. 5a.** Photomicrographs showing the oil-prone nature of investigated coals. 1) Fluorescing vitrinites
834 and liptinites in sample Ba1 from Bassen. 2) Fluorescing vitrinite groundmass with abundant micrinite
835 (fine granular white macerals interspersed on vitrinite), abundant liptodetrinite (Lpd) and bituminite – Bit
836 in sample L12 from Lunckefjellet. 3) Oil expulsion from crack on a collotelinite in sample L13 from
837 Lunckefjellet. 4) Fluorescing vitrinites in sample Br2 from Breinosa. C = collotelinite, Co = corpogelinite,
838 Cd = collodetrinite, R = resinite, Sp = Sporinite, Cu = cutinite, F = fusinite, Sf = semifusinite, In =
839 inertodetrinite, Fg = funginite. Black/white photo = normal light. Coloured photo = UV light.
840
841 **Fig. 5b.** Photomicrographs showing the oil-prone nature of investigated coals. 1) Cutinite (Cu), resinite
842 (R), sporinite (Sp) and liptodetrinite (Lpd) in a perhydrous collodetrinite (Cd) groundmass in sample Br4
843 from Breinosa. 2) Suberinite (Sb) cell walls are typically in-filled with fluorescing corpogelinites (Co) in
844 sample Br4 from Breinosa. 3) Oil expulsion from crack on perhydrous collodetrinite in sample Br4 from
845 Breinosa. 4) Detrovitrinite showing stronger fluorescence than collotelinite in sample C2 from
846 Colesdalen. Note: pyrite (P) framboids (diameter ~2 - 35 µm) in (1) and (2) are indicative of oxygen-
847 poor deposition associated with relatively high marine influence. R = resinite, Sf = semifusinite.
848 Black/white photo = normal light. Coloured photo = UV light.
849
850 **Fig. 6.** van Krevelen equivalent diagram of the CTB coals. The coals plot on the Type II kerogen line
851 and between the Types II and III kerogen lines despite being predominately composed of vitrinites.
852
853 **Fig. 7.** Rock-Eval 6 pyrogram (drawn to scale) showing multiple minor S2 peaks in sample Br4 from
854 Breinosa BH4-2009 locality. The multiple S2 peaks are possibly associated with the release of heavy,
855 liquid hydrocarbons volatilized at temperatures higher than normal for S1.
856
857 **Fig. 8a.** VR vs T_{max} plot for the CTB coals.
858

Fig. 8b. LoVR vs T_{max} plot for the CTB coals.

Fig. 8c. Rank(S_r) vs T_{max} plot for the CTB coals.

Fig. 8d. Rank(S_r) vs LoVR plot for the CTB coals.

Fig. 9a. LoVR vs HI plot for the CTB coals (after Petersen, 2006). Samples plotting to the left of and on the HI_{max} line are in stages i and ii petroleum generation respectively, while those plotting to the right of the HI_{max} line are in stage iii petroleum generation. Note: the HI_{max} line of the CTB coals shifts towards higher maturity compared to the world-wide coal data-set (shaded area) of Petersen (2006).

Fig. 9b. Rank(S_r) vs HI plot for the CTB coals (after Sykes and Snowdon, 2002). Note: the trend of the CTB coals parallels that of the NZ Coal Band (shaded area).

Fig. 9c. T_{max} vs HI plot for the CTB coals (after Sykes and Snowdon, 2002). Note: the trend of the CTB coals closely follows that of the NZ Coal Band (shaded area).

Fig. 10a. LoVR vs BI plot for the CTB coals under study (after Petersen, 2006). Note: the shaded area is the world-wide coal data-set of Petersen (2006).

Fig. 10b. T_{max} vs BI plot for the CTB coals (after Sykes and Snowdon, 2002). Note: the trend of the CTB coals parallels that of the NZ Coal Band (shaded area).

Fig. 10c. Rank(S_r) vs BI plot for the CTB coals (after Sykes and Snowdon, 2002). Note: the trend of the CTB coals closely follows that of the NZ Coal Band (shaded area).

Fig. 11. Comparing the S_T vs BI and S_T vs HI plots of the Bassen and Colesdalen coals to show the influence of sulphur in petroleum generation. Note: the positive correlation observed for Bassen is probably because oil expulsion has not started, while the negative relationship at Colesdalen is because the coals are already expelling oil.

889 **Fig. 12.** Sulphur profiles within seams and across sampled localities in the CTB. Note: the sizes of the
890 plots are proportional and reflect the relative seam thicknesses and S_T contents.
891
892 **Fig. 13.** A schematic N-S transect across an idealised Adventdalen section (i.e. from Bassen to Mine 7
893 to BH4-2009) showing the relationship between oil potential and marine influence. Note: Mine 7 data
894 are from Marshall et al. 2015a; Uguna, 2016.

895 **Table 1**

Sample ID	Area	Location and sample type	Seam	Drill depth (m)	Median sample position above seam base (m)	Core/sample length (m)
Ba1	Bassen	Outcrop section	Longyear	-	1.99	0.07
Ba2	Bassen	Outcrop section	Longyear	-	1.87	0.05
Ba3	Bassen	Outcrop section	Longyear	-	1.70	0.06
Ba4	Bassen	Outcrop section	Longyear	-	1.51	0.05
Ba5	Bassen	Outcrop section	Longyear	-	1.38	0.07
Ba6	Bassen	Outcrop section	Longyear	-	1.19	0.06
Ba7	Bassen	Outcrop section	Longyear	-	1.09	0.04
Ba8	Bassen	Outcrop section	Longyear	-	0.94	0.06
Ba9	Bassen	Outcrop section	Longyear	-	0.82	0.06
Ba10	Bassen	Outcrop section	Longyear	-	0.54	0.06
Ba11	Bassen	Outcrop section	Longyear	-	0.37	0.07
Ba12	Bassen	Outcrop section	Longyear	-	0.23	0.06
Ba13	Bassen	Outcrop section	Longyear	-	0.17	0.07
Ba14	Bassen	Outcrop section	Longyear	-	0.03	0.06
L1	Lunckefjellet	BH15-2011	Longyear	-258.30	2.10	0.10
L2	Lunckefjellet	BH15-2011	Longyear	-258.50	1.90	0.10
L3	Lunckefjellet	BH15-2011	Longyear	-258.80	1.60	0.10
L4	Lunckefjellet	BH15-2011	Longyear	-259.00	1.40	0.10
L5	Lunckefjellet	BH15-2011	Longyear	-259.20	1.20	0.10
L6	Lunckefjellet	BH15-2011	Longyear	-259.40	1.00	0.10
L7	Lunckefjellet	BH15-2011	Longyear	-259.60	0.80	0.10
L8	Lunckefjellet	BH15-2011	Longyear	-259.80	0.60	0.10
L9	Lunckefjellet	BH15-2011	Longyear	-260.10	0.30	0.10
L10	Lunckefjellet	BH15-2011	Longyear	-260.30	0.10	0.10
L11	Lunckefjellet	BH10-2009	Longyear	-69.71	0.79	0.30
L12	Lunckefjellet	BH10-2009	Longyear	-69.97	0.53	0.22
L13	Lunckefjellet	BH10-2009	Longyear	-70.19	0.32	0.21
L14	Lunckefjellet	BH10-2009	Longyear	-70.40	0.11	0.21
L15	Lunckefjellet	BH10-2007	Longyear	-247.06	1.49	0.25
L16	Lunckefjellet	BH10-2007	Longyear	-247.31	1.24	0.25
L17	Lunckefjellet	BH10-2007	Longyear	-247.56	0.99	0.25
L18	Lunckefjellet	BH10-2007	Longyear	-248.06	0.49	0.25
L19	Lunckefjellet	BH10-2007	Longyear	-248.45	0.10	0.19
L20	Lunckefjellet	BH6A-2007	Longyear	-223.03	1.88	0.25
L21	Lunckefjellet	BH6A-2007	Longyear	-223.78	1.13	0.25
Br1	Breinosa	BH4-2009	Longyear	-314.73	1.16	0.20
Br2	Breinosa	BH4-2009	Longyear	-314.94	0.96	0.21
Br3	Breinosa	BH4-2009	Longyear	-315.15	0.75	0.21
Br4	Breinosa	BH4-2009	Longyear	-315.65	0.24	0.16
Br5	Breinosa	BH4-2009	Longyear	-315.81	0.08	0.16
C1	Colesdalen	BH3-2008	Verkhnij	-274.13	1.73	0.25
C2	Colesdalen	BH3-2008	Verkhnij	-274.38	1.48	0.25
C3	Colesdalen	BH3-2008	Verkhnij	-274.63	1.23	0.25
C4	Colesdalen	BH3-2008	Verkhnij	-275.05	0.81	0.23
C5	Colesdalen	BH3-2008	Verkhnij	-275.28	0.58	0.23
C6	Colesdalen	BH3-2008	Verkhnij	-275.51	0.35	0.23
C7	Colesdalen	BH3-2008	Verkhnij	-275.74	0.12	0.23

896

Table 2

Sample ID	Maceral composition (vol % mmf)																	Maturity parameters		
	Tel	Clt	Cld	Vtd	Cpg	F	Sf	Fg	Mac	Mic	In	Sp	Cut	Res	Bit	Sb	Lpd	VR	LoVR	Rank(S_r)
Ba1	0.0	58.8	24.0	4.8	2.4	0.0	2.0	1.6	0.0	0.0	1.6	0.8	1.6	2.0	0.0	0.0	0.4	0.54	0.66	-
Ba2	0.4	67.1	17.5	4.5	4.1	0.4	0.0	2.4	0.0	0.0	2.0	0.4	0.0	0.8	0.0	0.0	0.4	0.59	0.68	-
Ba3	0.2	56.6	25.3	6.9	6.3	0.2	0.6	1.2	0.0	0.0	0.4	0.2	0.6	1.2	0.0	0.0	0.4	0.59	0.70	-
Ba4	0.0	68.5	17.8	3.4	7.1	0.4	0.0	0.6	0.0	0.0	0.4	0.8	0.6	0.0	0.0	0.0	0.4	0.59	0.67	-
Ba5	3.6	74.5	15.0	1.2	1.2	0.0	0.8	0.8	0.0	0.0	1.2	0.4	0.8	0.0	0.0	0.0	0.4	0.59	0.65	-
Ba6	1.2	78.9	10.9	2.2	1.6	0.0	0.8	0.8	0.0	0.2	1.6	0.0	0.4	0.0	0.0	0.0	1.2	0.62	0.70	-
Ba7	0.0	56.7	27.9	3.2	6.1	0.4	0.0	1.2	0.0	0.0	1.2	0.4	1.2	1.6	0.0	0.0	0.0	0.56	0.65	-
Ba8	0.0	63.1	22.9	3.2	5.6	0.4	1.2	0.8	0.0	0.0	0.4	0.8	0.0	0.8	0.0	0.0	0.8	0.62	0.71	-
Ba9	5.0	69.2	12.7	3.6	0.0	0.5	2.7	1.8	0.0	0.0	1.4	1.4	1.4	0.0	0.0	0.0	0.5	0.68	0.73	-
Ba10	0.8	55.3	26.0	5.3	0.4	0.0	3.7	3.3	0.0	0.0	3.7	0.8	0.0	0.4	0.0	0.0	0.4	0.65	0.70	-
Ba11	3.3	73.7	10.3	1.6	0.8	2.1	3.3	0.8	0.0	0.0	1.6	0.0	0.0	0.8	0.0	0.0	1.6	0.65	0.69	-
Ba12	0.4	59.7	23.0	5.2	2.0	1.2	0.0	4.0	0.0	0.0	0.4	1.6	0.8	0.8	0.0	0.0	0.8	0.57	0.66	-
Ba13	2.1	70.4	12.4	2.5	2.5	0.8	0.8	1.7	0.0	0.4	0.4	0.8	0.4	2.5	0.0	0.0	2.1	0.61	0.69	-
Ba14	0.0	74.0	19.6	0.6	0.8	0.0	0.8	0.8	0.0	0.2	0.4	0.8	0.4	1.2	0.0	0.0	0.4	0.63	0.70	-
L1	0.8	57.3	29.2	0.2	5.4	0.0	0.0	1.6	0.0	0.2	0.8	0.6	1.0	2.0	0.0	0.0	0.8	0.59	0.72	9.1
L2	2.1	48.5	28.9	4.2	7.5	2.5	1.3	0.8	0.0	0.0	1.3	0.0	1.3	0.4	0.0	0.0	1.3	0.64	0.77	12.4
L3	0.2	38.8	33.6	3.4	2.4	0.6	10.9	1.5	0.0	0.4	2.8	0.9	0.6	1.7	0.0	0.0	2.1	0.60	0.76	11.6
L4	2.0	44.9	33.6	6.5	8.9	0.4	0.0	0.8	0.0	0.4	0.8	0.4	0.4	0.4	0.0	0.0	0.4	0.62	0.79	9.8
L5	0.4	42.5	34.8	2.8	7.7	1.6	1.2	2.8	0.4	0.4	2.4	0.0	0.0	1.6	0.0	0.0	1.2	0.61	0.81	11.2
L6	2.4	70.9	12.1	0.2	0.8	0.2	2.0	4.0	0.0	0.0	2.4	0.8	1.2	1.6	0.0	0.0	1.2	0.58	0.77	10.4
L7	0.0	60.2	18.8	10.8	2.8	0.0	2.3	0.6	0.0	0.0	2.3	0.0	0.6	0.6	0.0	0.0	1.1	0.70	0.85	13.3
L8	0.8	47.5	26.6	5.7	6.6	1.2	4.1	0.4	0.0	0.0	1.2	0.0	0.8	2.5	0.0	0.0	2.5	0.68	0.84	7.0
L9	0.0	59.6	29.4	0.8	2.9	0.0	0.4	0.0	0.0	0.4	1.2	0.4	1.6	2.0	0.0	0.0	1.2	0.60	0.80	3.8
L10	0.4	62.4	25.2	2.1	0.8	0.0	0.0	0.8	0.0	0.4	0.0	0.0	2.5	2.5	0.0	0.0	2.9	0.63	0.81	3.7
L11	0.0	49.7	31.0	8.3	0.0	1.1	4.8	1.1	0.0	0.3	1.6	0.5	1.1	0.5	0.0	0.0	0.0	0.61	0.78	13.1
L12	3.7	70.4	18.0	2.4	1.2	0.0	0.8	0.0	0.0	0.0	1.2	0.4	0.8	0.8	0.2	0.0	0.0	0.73	0.80	9.7
L13	3.7	67.1	14.6	3.9	0.4	0.0	7.3	0.4	0.0	0.2	1.2	0.0	0.4	0.0	0.0	0.0	0.8	0.75	0.81	10.0
L14	0.0	62.3	23.0	4.1	1.2	1.6	4.9	0.0	0.0	0.4	0.8	0.0	0.8	0.8	0.0	0.0	0.0	0.68	0.80	11.1
L15	0.0	57.9	21.5	6.1	6.5	0.4	1.6	1.6	0.0	0.0	0.8	1.2	0.4	1.2	0.0	0.0	0.8	0.58	0.77	10.8
L16	0.4	51.8	27.3	3.3	10.2	0.8	0.4	0.8	0.0	0.0	2.0	0.0	0.0	2.0	0.0	0.0	0.8	0.59	0.75	10.0
L17	1.2	50.4	31.8	2.9	9.5	0.0	0.0	0.4	0.0	0.8	0.0	0.0	0.4	0.4	0.0	0.0	2.1	0.64	0.77	9.5
L18	1.8	52.6	27.6	6.1	6.1	0.0	0.9	0.9	0.0	0.4	0.0	0.4	0.0	0.4	0.0	0.0	2.6	0.71	0.81	9.7
L19	1.6	40.8	46.1	4.2	0.5	0.5	2.1	0.5	0.0	0.5	0.5	0.0	0.5	1.0	0.0	0.0	1.0	0.64	0.79	13.7
L20	0.4	29.3	38.2	14.2	9.8	0.4	1.6	1.6	0.0	0.8	0.4	0.0	0.8	1.2	0.0	0.0	1.2	0.58	0.68	8.1
L21	2.4	43.5	26.6	8.1	9.3	1.2	2.0	2.0	0.0	0.4	0.8	0.4	0.8	1.2	0.0	0.0	1.2	0.67	0.78	9.0
Br1	0.0	32.4	54.8	2.9	2.4	0.5	0.5	0.0	0.0	1.9	1.4	0.5	0.0	1.9	0.0	0.0	1.0	0.60	0.76	13.8
Br2	0.0	67.4	22.3	3.3	0.8	0.0	1.7	1.2	0.0	0.4	1.7	0.0	0.4	0.8	0.0	0.0	0.0	0.66	0.84	12.6
Br3	1.8	75.4	13.6	4.8	1.5	0.0	1.3	0.4	0.0	0.0	0.0	0.4	0.0	0.4	0.0	0.0	0.2	0.69	0.81	12.5
Br4	0.0	59.5	26.5	1.9	0.0	0.2	7.1	0.0	0.0	0.0	0.0	0.0	2.1	1.9	0.0	0.2	0.5	0.66	0.83	13.7
Br5	1.3	57.3	33.8	4.5	0.0	0.0	0.0	0.0	0.0	0.0	1.9	0.6	0.0	0.6	0.0	0.0	0.0	0.59	0.78	14.1
C1	1.0	57.9	14.6	2.9	0.8	1.2	16.5	0.0	0.0	0.0	1.9	0.8	0.8	1.0	0.0	0.0	0.4	0.77	0.88	13.4
C2	1.2	60.0	13.4	6.9	1.0	5.7	7.5	0.0	0.0	0.0	1.6	0.6	0.4	1.0	0.0	0.0	0.6	0.79	0.90	13.6
C3	0.9	65.2	11.4	3.0	0.0	1.7	13.8	0.0	0.2	0.0	1.9	0.9	0.2	0.6	0.0	0.0	0.2	0.79	0.90	13.9
C4	0.0	64.6	12.8	3.7	0.0	1.8	11.0	0.0	0.0	0.0	4.9	0.6	0.0	0.6	0.0	0.0	0.0	0.65	0.77	14.7
C5	0.0	58.5	11.0	0.8	0.0	1.2	22.8	0.0	0.0	0.0	3.3	1.6	0.4	0.0	0.0	0.0	0.4	0.78	0.89	12.9
C6	0.0	78.1	7.6	1.2	0.0	0.6	9.9	0.4	0.0	0.0	1.4	0.0	0.2	0.2	0.0	0.0	0.2	0.80	0.93	13.4
C7	0.4	59.1	18.1	0.8	0.0	1.6	15.0	0.2	0.2	0.0	3.5	0.2	0.4	0.2	0.0	0.0	0.2	0.76	0.89	13.3

899 **Table 3**

Sample ID	S1 (mg/g)	S2 (mg/g)	T_{max} (°C)	TOC (%)	HI	OI	PI	BI	H	Soxhlet yield (mg/g)	S_T (%)	Fe (%)	Fe/S	Ash (%)	VM (%)	CV (Btu/lb)
Ba1	11.0	212.6	429	75.4	282	26	0.05	14.6	5.5	109.6	1.46	0.28	0.19	1.4	-	-
Ba2	7.9	171.3	429	74.2	231	28	0.04	10.7	5.2	91.7	1.51	0.73	0.48	1.3	-	-
Ba3	8.6	186.7	430	74.8	250	29	0.04	11.4	5.2	84.7	1.14	0.48	0.43	1.4	-	-
Ba4	6.0	168.5	431	73.9	228	31	0.03	8.1	5.4	101.9	0.80	0.44	0.55	1.3	-	-
Ba5	5.0	140.6	433	72.4	194	38	0.03	6.9	5.1	90.9	0.69	0.65	0.94	2.8	-	-
Ba6	5.1	141.9	426	65.5	217	39	0.03	7.7	5.2	97.1	0.57	0.67	1.17	1.0	-	-
Ba7	7.7	178.0	428	74.0	240	37	0.04	10.4	5.4	94.4	0.54	0.29	0.55	2.1	-	-
Ba8	5.7	146.4	437	71.0	206	38	0.04	8.0	5.0	82.8	0.54	0.58	1.07	1.1	-	-
Ba9	3.9	109.1	425	71.3	153	33	0.03	5.4	4.8	66.2	0.59	2.95	5.00	5.3	-	-
Ba10	5.8	129.6	425	74.7	174	42	0.04	7.8	4.9	76.5	0.62	0.42	0.68	1.3	-	-
Ba11	5.6	110.8	430	73.6	151	35	0.05	7.6	4.8	78.6	0.66	0.87	1.32	2.2	-	-
Ba12	7.0	165.1	429	74.6	221	32	0.04	9.4	5.4	81.1	0.84	0.33	0.39	2.0	-	-
Ba13	8.7	172.2	430	75.0	230	32	0.05	11.5	5.2	98.0	0.63	-	-	1.8	-	-
Ba14	7.5	144.9	432	75.3	192	32	0.05	10.0	5.1	90.4	0.96	0.40	0.42	1.6	-	-
L1	6.5	188.5	432	70.0	269	26	0.03	9.3	-	86.2	1.99	1.02	0.51	4.1	36.7	12852
L2	8.2	192.0	431	71.2	270	4	0.04	11.4	-	78.1	2.91	0.99	0.34	11.6	36.7	12852
L3	11.2	261.7	439	71.7	365	4	0.04	15.7	-	112.4	1.83	0.73	0.40	6.3	39.3	13651
L4	8.2	249.2	439	68.8	362	5	0.03	11.9	-	102.9	1.12	0.35	0.32	0.9	39.9	13651
L5	16.6	368.4	431	89.8	410	5	0.04	18.5	-	120.8	0.57	0.70	1.24	2.7	39.9	14137
L6	14.3	354.5	432	89.7	395	3	0.04	16.0	-	120.8	0.57	0.62	1.09	2.5	41.3	13942
L7	4.6	136.0	432	44.5	306	5	0.03	10.4	-	54.5	1.90	2.39	1.26	33.3	39.2	12534
L8	9.2	296.3	432	89.1	333	3	0.03	10.3	-	97.0	0.53	0.49	0.92	1.8	37.7	12637
L9	10.1	340.7	432	88.5	385	6	0.03	11.4	-	92.7	0.84	0.41	0.49	2.8	39.0	11502
L10	9.7	335.7	434	89.1	377	6	0.03	10.9	-	87.6	0.71	0.38	0.53	2.3	33.3	11775
L11	13.2	228.3	435	67.8	337	4	0.05	19.4	-	111.8	6.89	5.64	0.82	13.8	36.0	12133
L12	9.2	229.8	435	78.2	310	5	0.04	11.8	-	105.0	1.19	0.56	0.47	5.1	36.1	12966
L13	8.5	225.2	433	79.2	291	5	0.04	10.7	-	93.4	1.06	0.38	0.36	3.5	35.4	13356
L14	13.2	226.9	435	79.4	286	6	0.05	16.6	-	126.4	2.11	1.16	0.55	4.4	36.0	13432
L15	15.6	271.8	432	79.9	340	7	0.05	19.5	-	153.0	1.19	-	-	3.9	41.6	13847
L16	12.3	231.2	434	78.8	310	9	0.05	15.6	-	114.7	0.73	-	-	2.6	41.0	13662
L17	13.7	224.6	435	80.0	281	13	0.06	17.1	-	120.3	0.62	-	-	2.1	38.4	13392
L18	9.3	168.0	438	74.0	227	14	0.05	12.6	-	84.3	1.29	-	-	7.3	34.8	12628
L19	12.4	195.0	434	69.2	282	0	0.06	18.0	-	74.8	9.97	-	-	17.6	32.6	11203
L20	8.7	182.0	432	74.4	245	26	0.05	11.7	-	112.1	1.05	0.54	0.51	4.3	41.0	12667
L21	9.0	194.1	433	76.5	254	16	0.04	11.8	-	78.1	0.46	0.52	1.14	4.8	39.1	12867
Br1	13.3	212.5	444	65.7	324	1	0.06	20.3	-	69.6	6.89	-	-	19.8	33.5	11743
Br2	19.9	282.3	447	82.2	343	2	0.07	24.1	-	71.2	2.25	-	-	7.8	39.9	14142
Br3	15.6	207.6	439	71.0	292	2	0.07	22.0	-	55.0	1.91	-	-	16.5	38.1	12851
Br4	13.1	243.3	442	73.5	331	1	0.05	17.9	-	79.2	7.04	-	-	11.6	35.9	12957
Br5	10.8	200.3	442	57.1	351	1	0.05	19.0	-	50.3	6.81	-	-	29.5	30.2	10368
C1	15.0	206.8	442	83.1	249	2	0.07	18.1	-	100.0	2.26	1.35	0.60	3.9	32.2	14246
C2	13.2	204.9	443	80.0	256	2	0.06	16.6	-	143.2	1.84	0.82	0.45	7.3	32.6	13953
C3	12.4	185.4	443	72.0	258	1	0.06	17.2	-	44.4	2.01	1.01	0.50	16.6	29.2	12458
C4	12.8	159.2	440	58.7	271	0	0.07	21.9	-	42.3	12.05	10.24	0.85	24.4	29.8	11390
C5	18.4	208.4	443	86.2	242	2	0.08	21.3	-	59.5	1.67	0.31	0.19	1.9	32.1	14520
C6	19.0	230.3	442	86.3	267	1	0.08	22.0	-	69.4	1.39	0.39	0.28	5.1	33.7	14329
C7	15.7	218.2	445	82.3	265	1	0.07	19.1	-	71.8	1.87	1.15	0.61	5.0	34.1	14234

900 **Fig. 1**

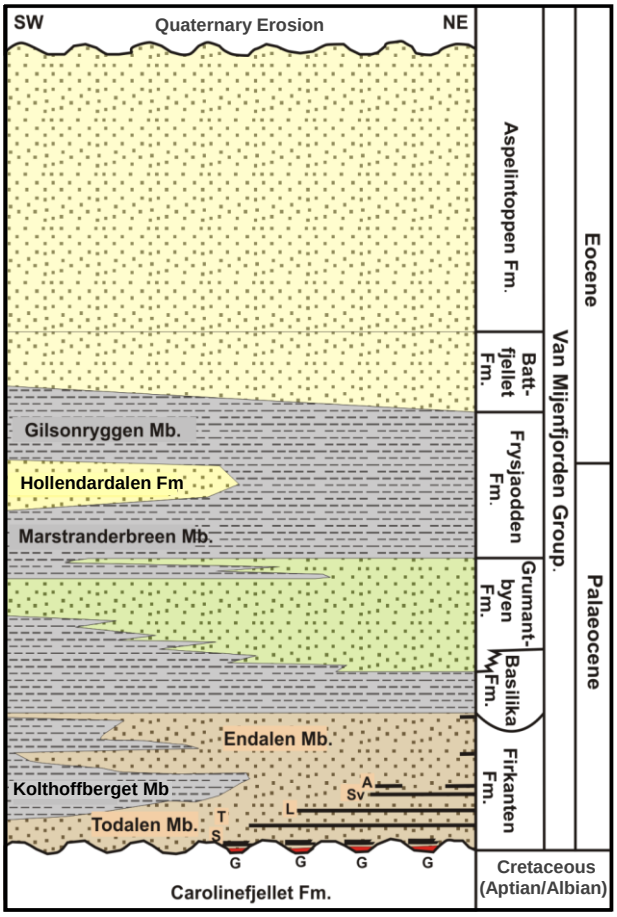
SW
Quaternary Erosion
NE
Aspelintoppen Fm.
Batt-fjellet Fm.
Gilsonryggen Mb.
Hollendardalen Fm
Marstranderbreen Mb.
Frysjaodden Fm.
Grumant-byen Fm.
Basilika Fm.
Endalen Mb.
Kolthoffberget Mb
Todalen Mb.
Firkanten Fm.
A
Sv
L
T
S
G
G
G
G
Carolinefjellet Fm.
Van Mijenfjorden Group.
Eocene
Palaeocene
Cretaceous (Aptian/Albian)

901

902 **Fig. 2**

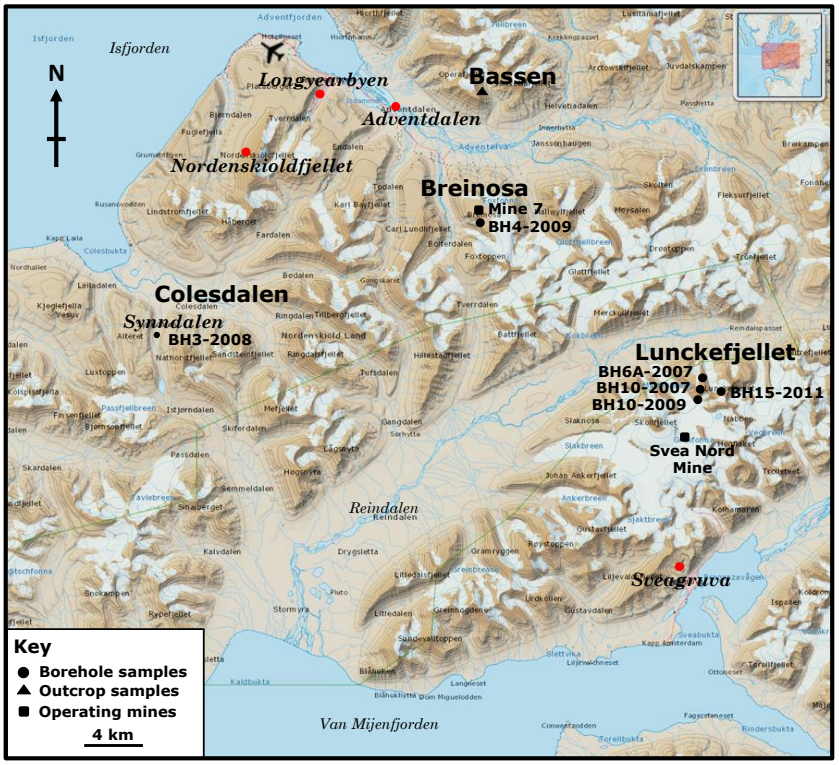
Isfjorden
N
Longyearbyen
Bassen
Adventdalen
Nordenskioldfjellet
Breinosa
Mine 7
BH4-2009
Colesdalen
Synndalen
BH3-2008
Lunckefjellet
BH6A-2007
BH10-2007
BH10-2009
BH15-2011
Svea Nord
Mine
Reindalen
Sveagruva
Van Mijenfjorden
Key
Borehole samples
Outcrop samples
Operating mines
4 km

903

904 **Fig. 3**

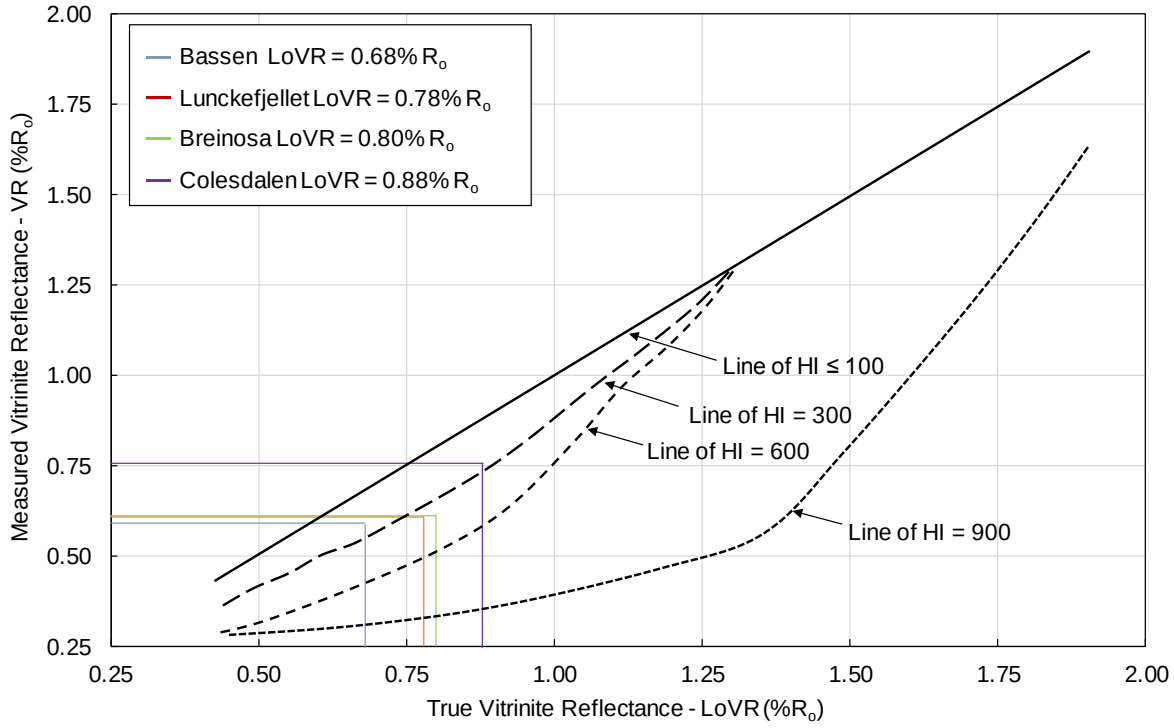

905

906

907 **Fig. 4**

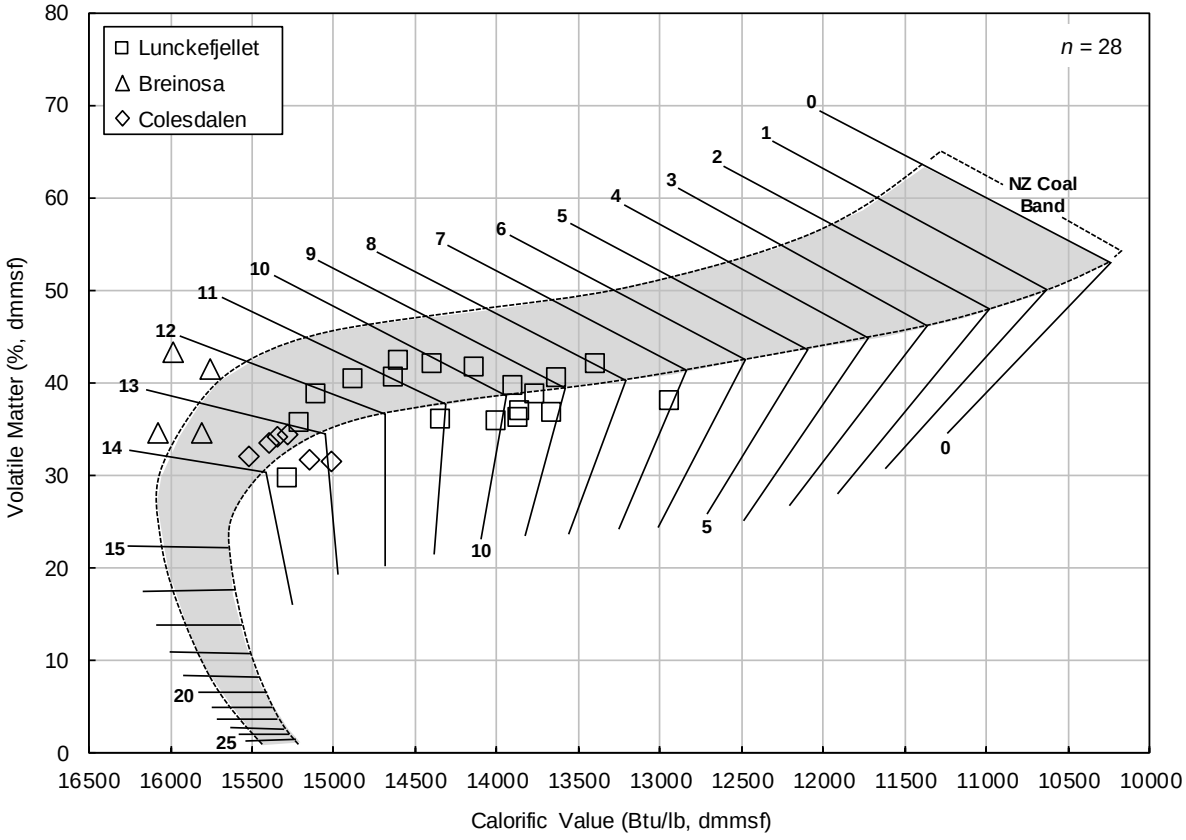
Lunckefjellet
Breinosa
Colesdalen
n = 28
NZ Coal Band
0
1
2
3
4
5
6
7
8
9
10
11
12
13
14
15
20
25
0
5
10
Volatile Matter (%, dmmsf)
Calorific Value (Btu/lb, dmmsf)
80
70
60
50
40
30
20
10
0
16500
16000
15500
15000
14500
14000
13500
13000
12500
12000
11500
11000
10500
10000

908

Fig. 5a

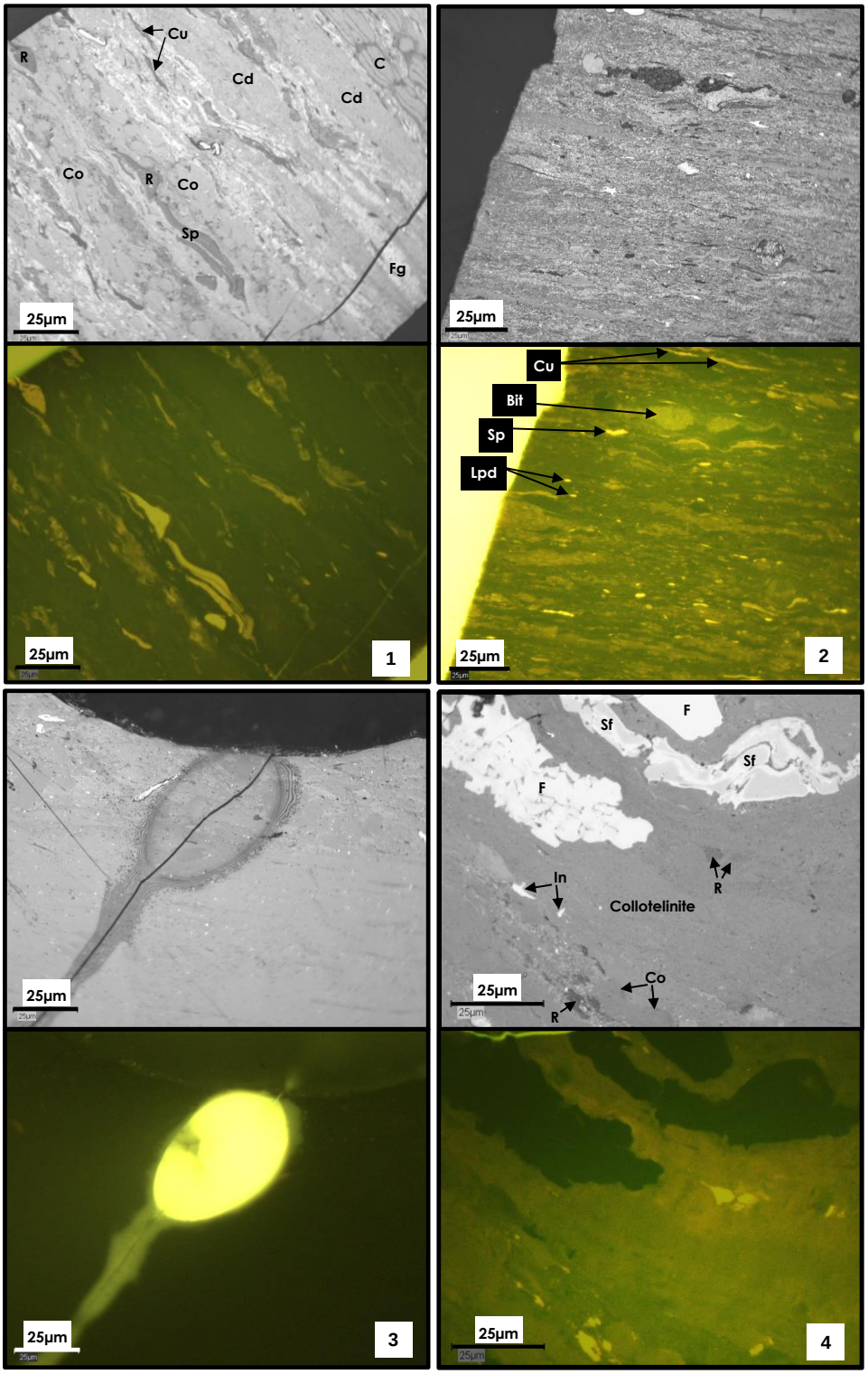
Cu
R
Cd
C
Cd
Co
R
Co
Sp
Fg
25µm
25µm
Cu
Bit
Sp
Lpd
25µm
1
25µm
2
25µm
F
Sf
Sf
F
In
R
Collotelinite
25µm
Co
R
25µm
3
25µm
4

911 **Fig. 5b**

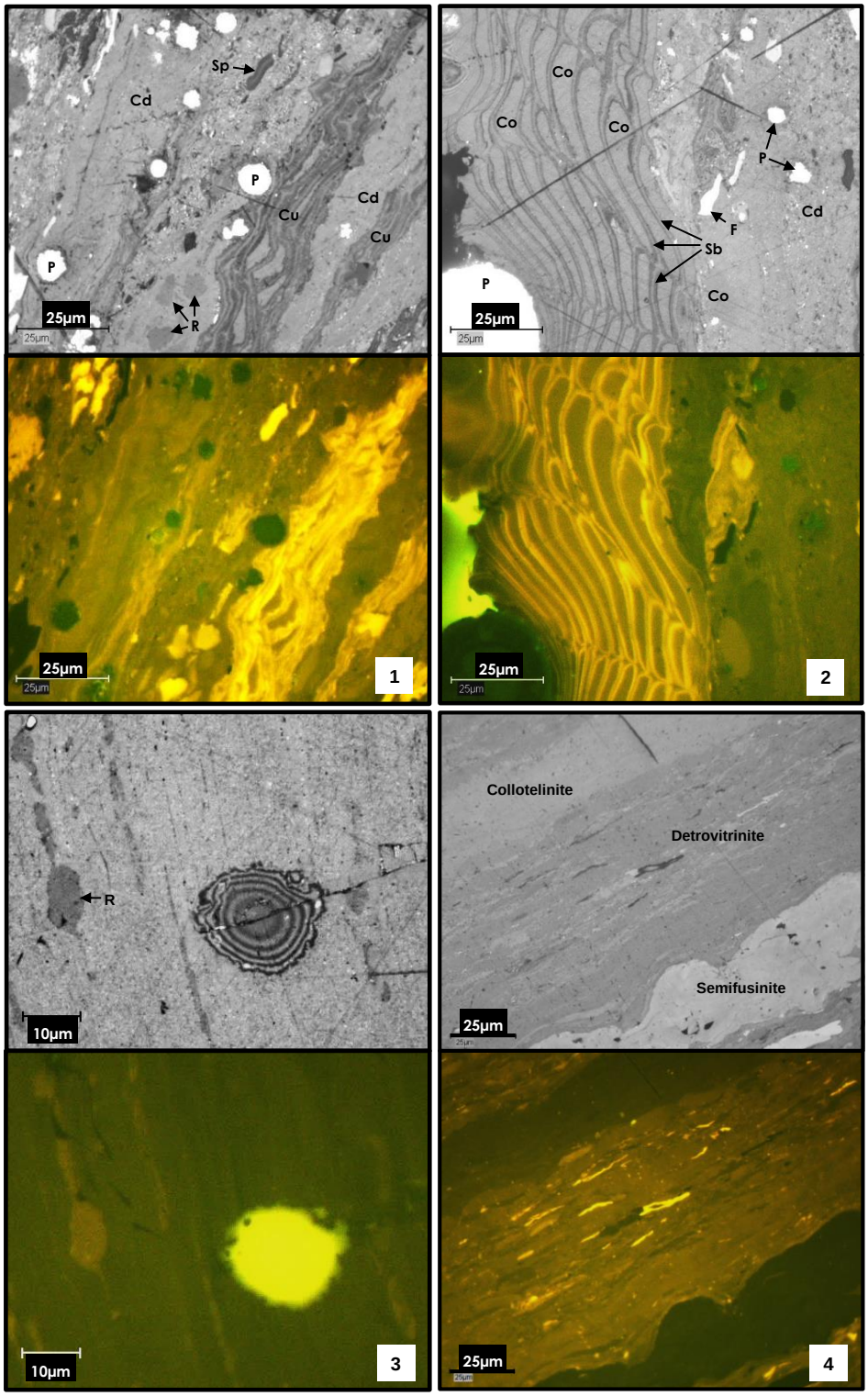

912

913 **Fig. 6**

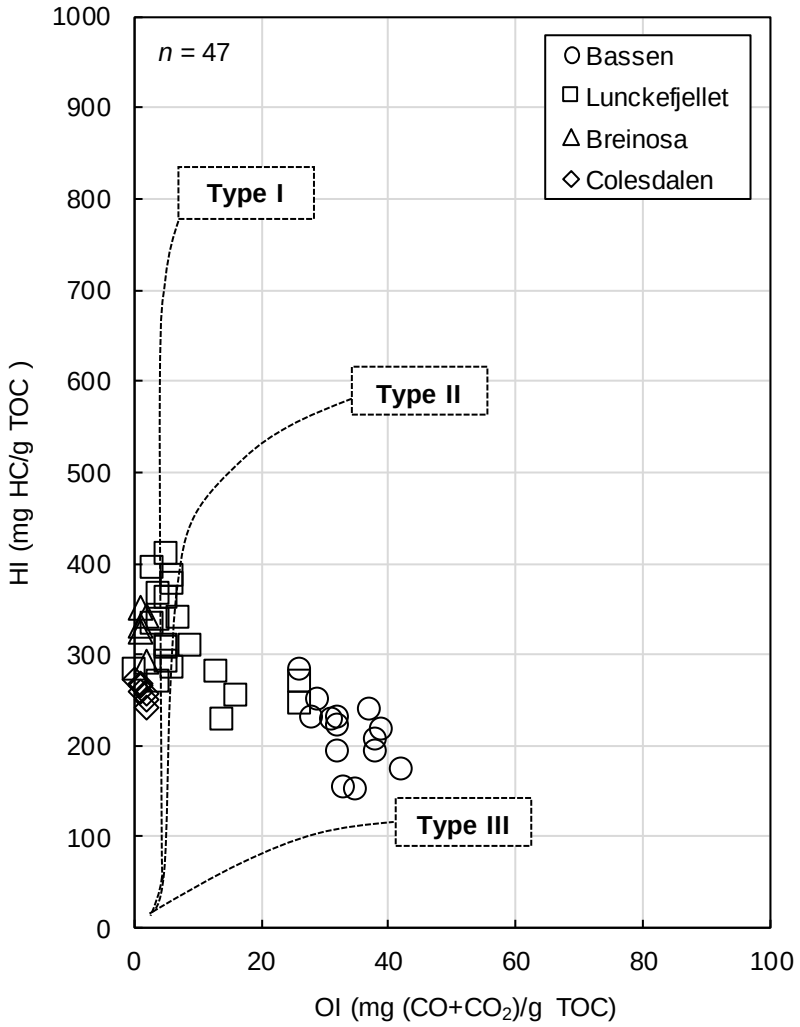
n = 47
Bassen
Lunckefjellet
Breinosa
Colesdalen
Type I
Type II
Type III
HI (mg HC/g TOC)
OI (mg (CO+CO2)/g TOC)
0
100
200
300
400
500
600
700
800
900
1000
0
20
40
60
80
100

914

915 **Fig. 7**

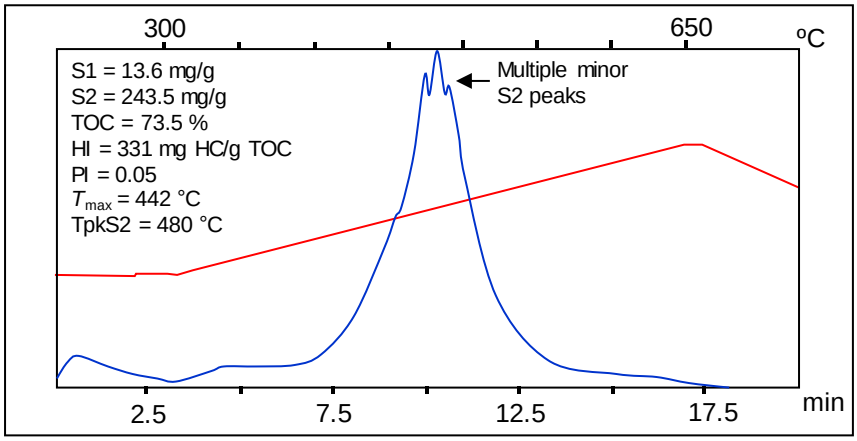

916

917

Fig. 8a

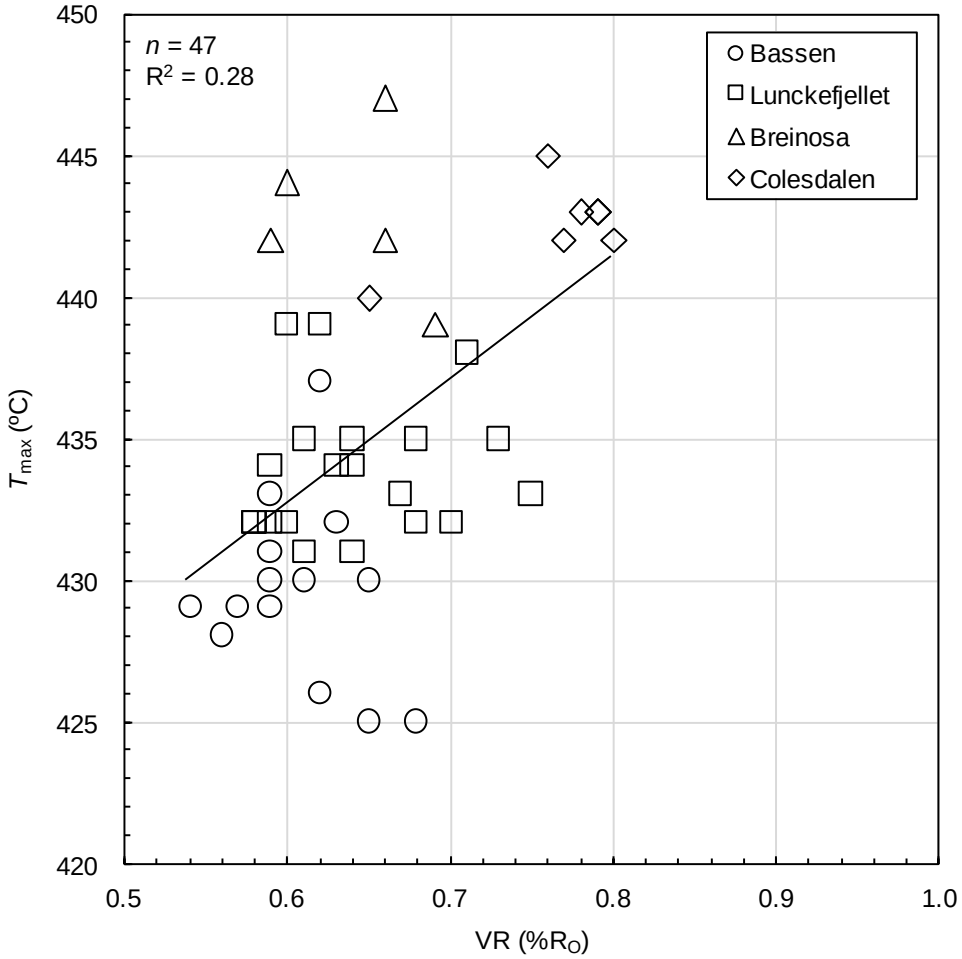
n = 47
R2 = 0.28
Bassen
Lunckefjellet
Breinosa
Colesdalen
Tmax (ºC)
VR (%RO)
450
445
440
435
430
425
420
0.5
0.6
0.7
0.8
0.9
1.0

Fig. 8b

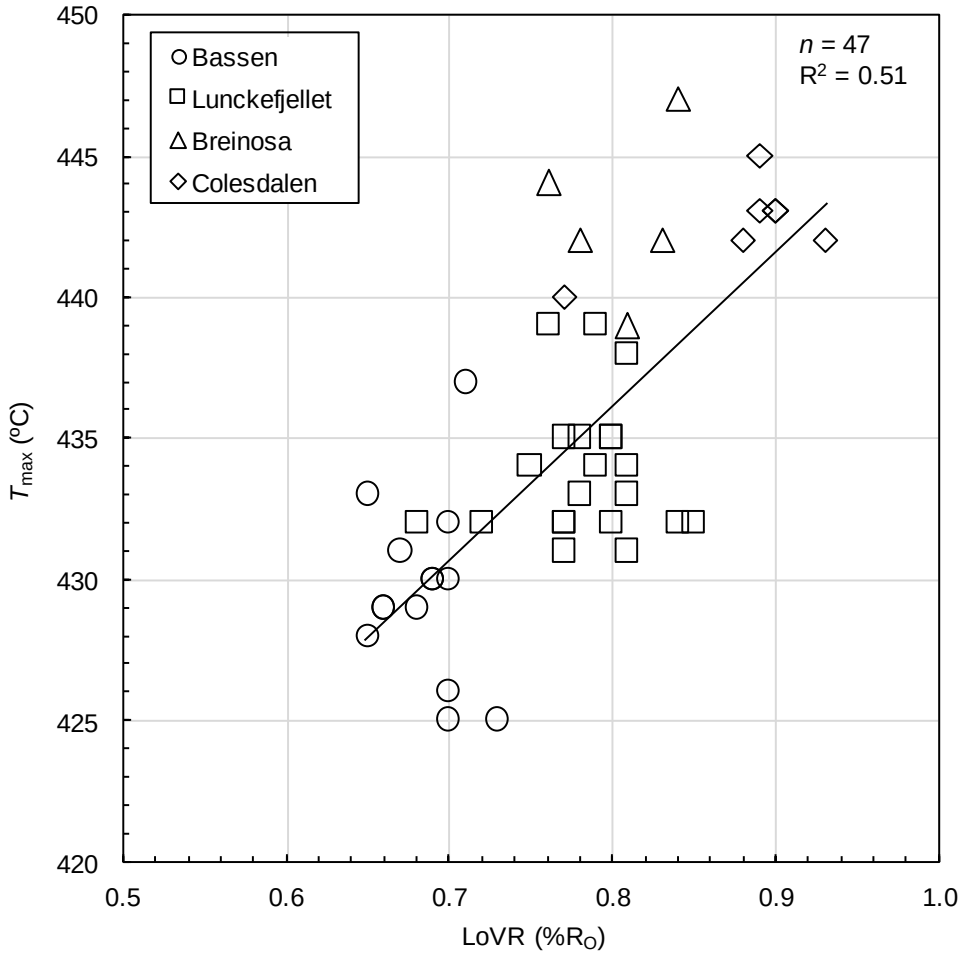
Bassen
Lunckefjellet
Breinosa
Colesdalen
n = 47
R2 = 0.51
Tmax (ºC)
LoVR (%RO)
450
445
440
435
430
425
420
0.5
0.6
0.7
0.8
0.9
1.0

923 **Fig. 8c**

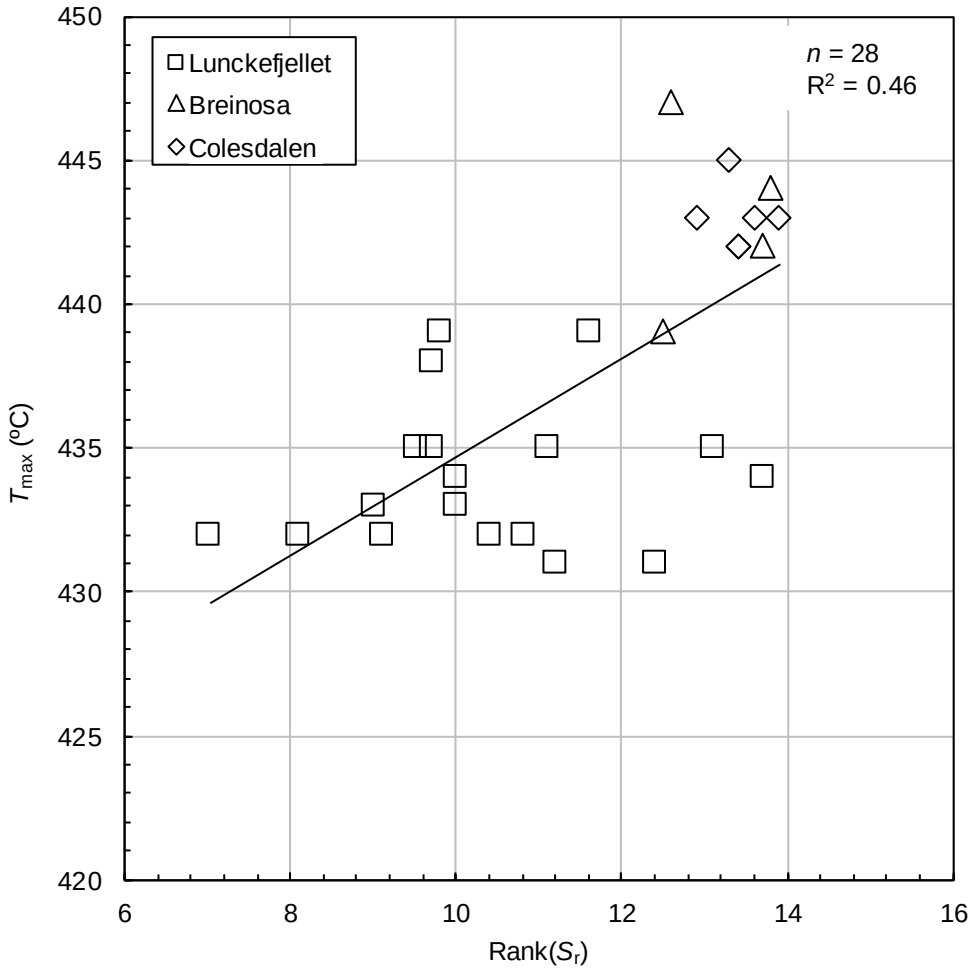

924

925

926 **Fig. 8d**

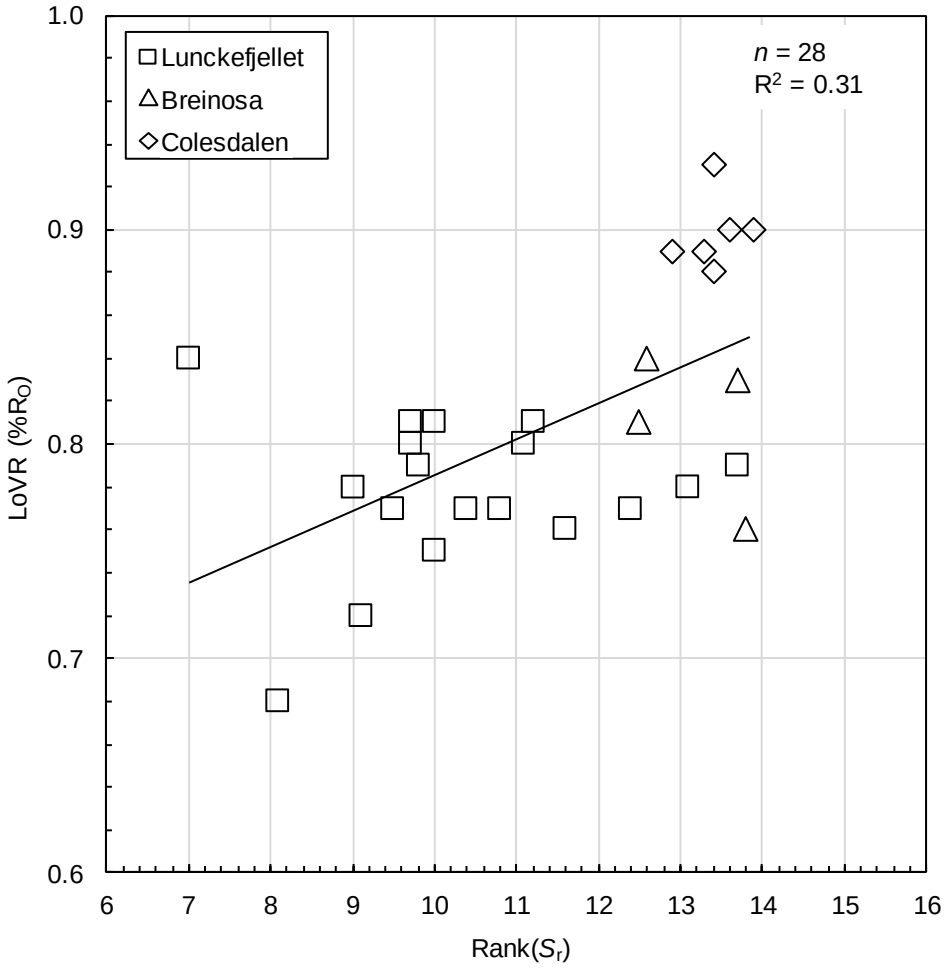

927

928 **Fig. 9a**

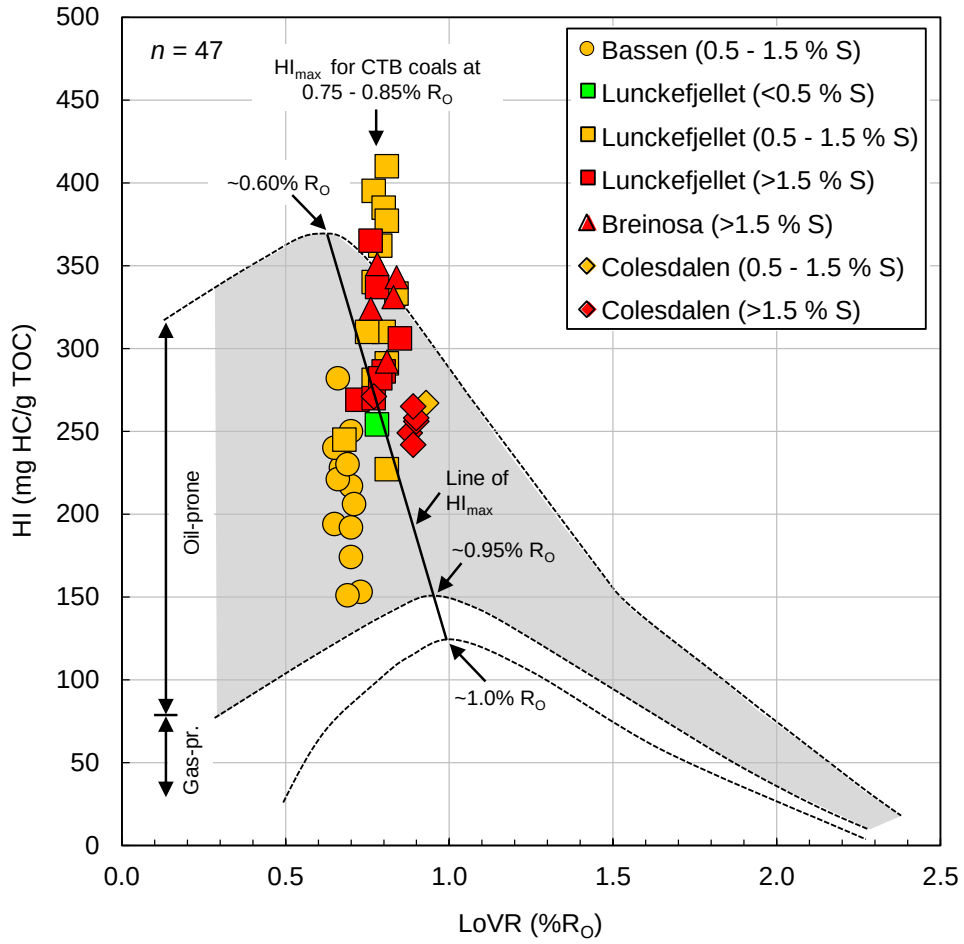

929

930 **Fig. 9b**

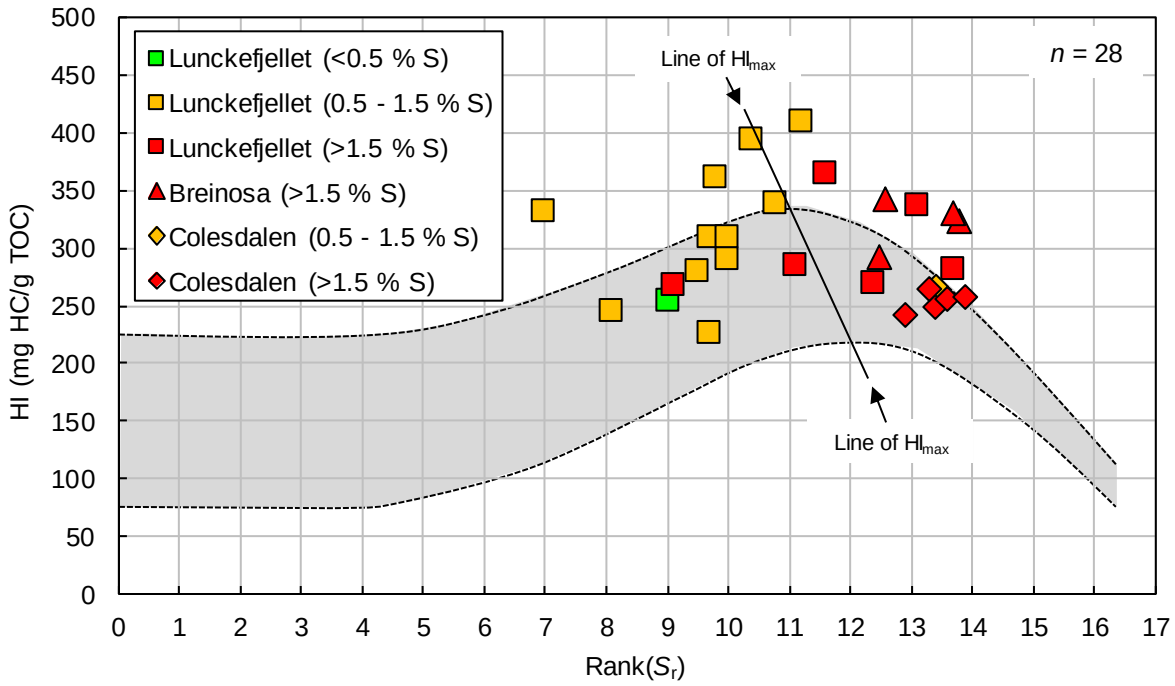

931

932

933 **Fig. 9c**

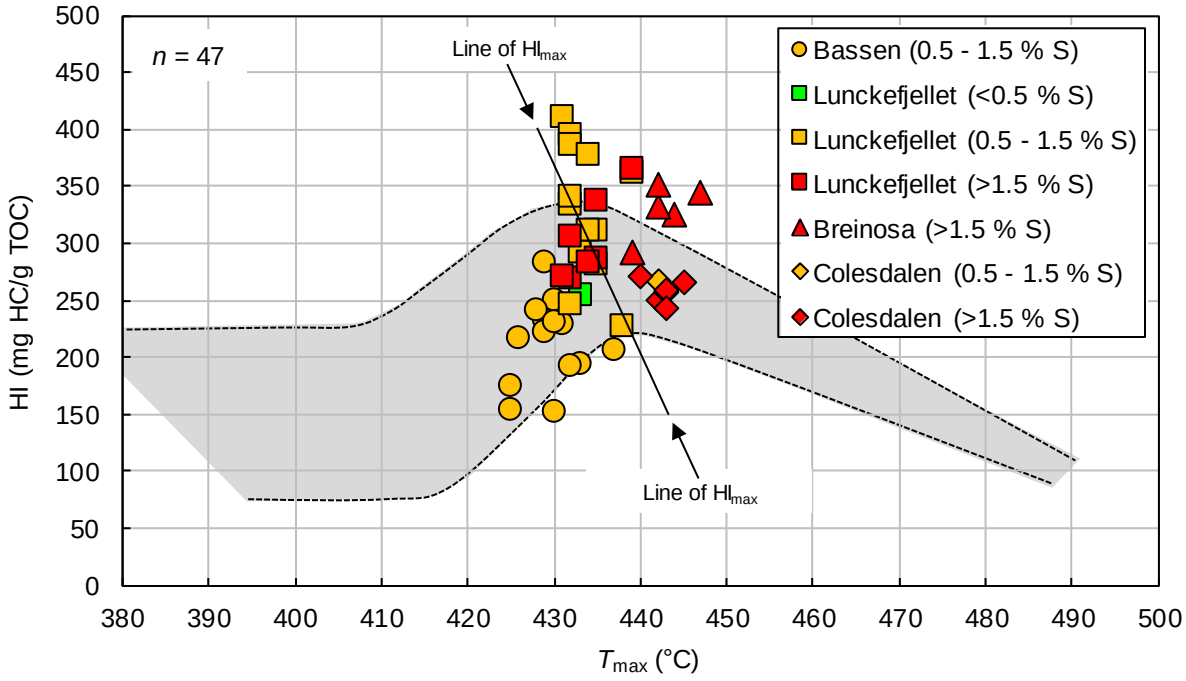

934

935

936 **Fig. 10a**

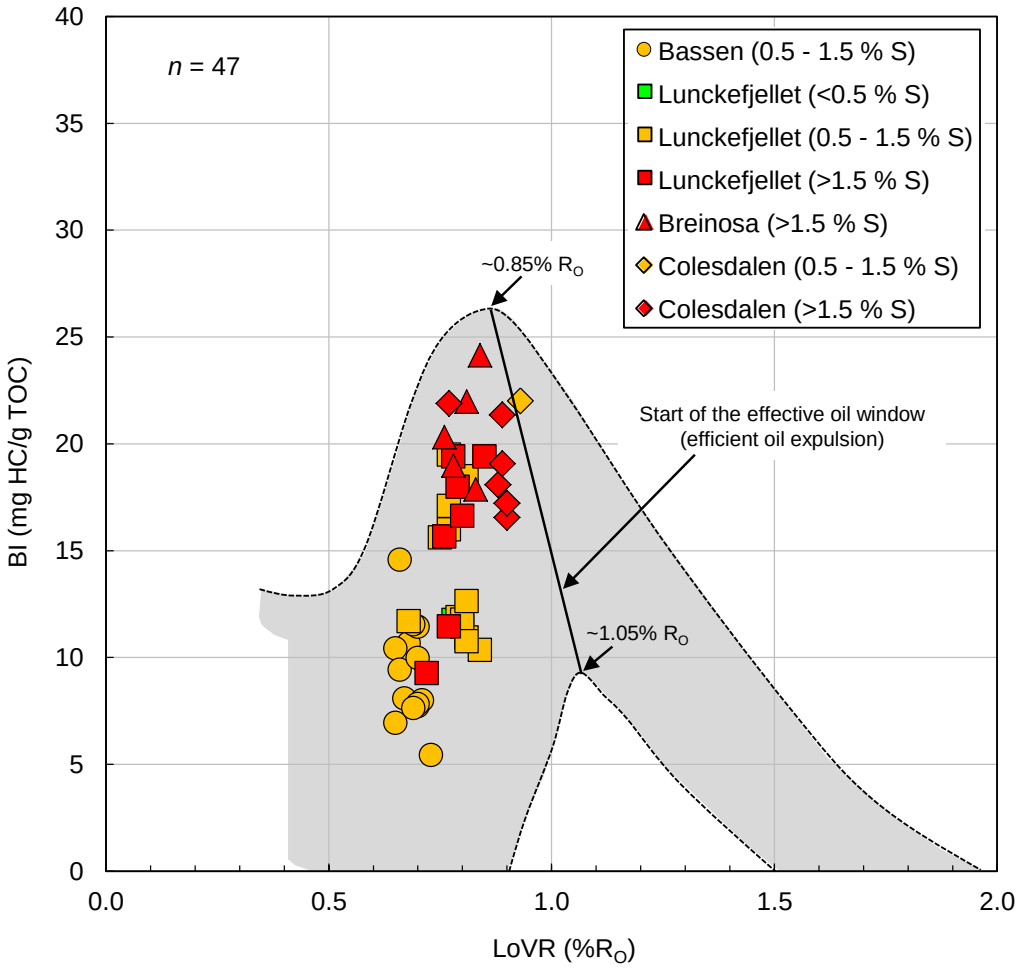

937

938 **Fig. 10b**

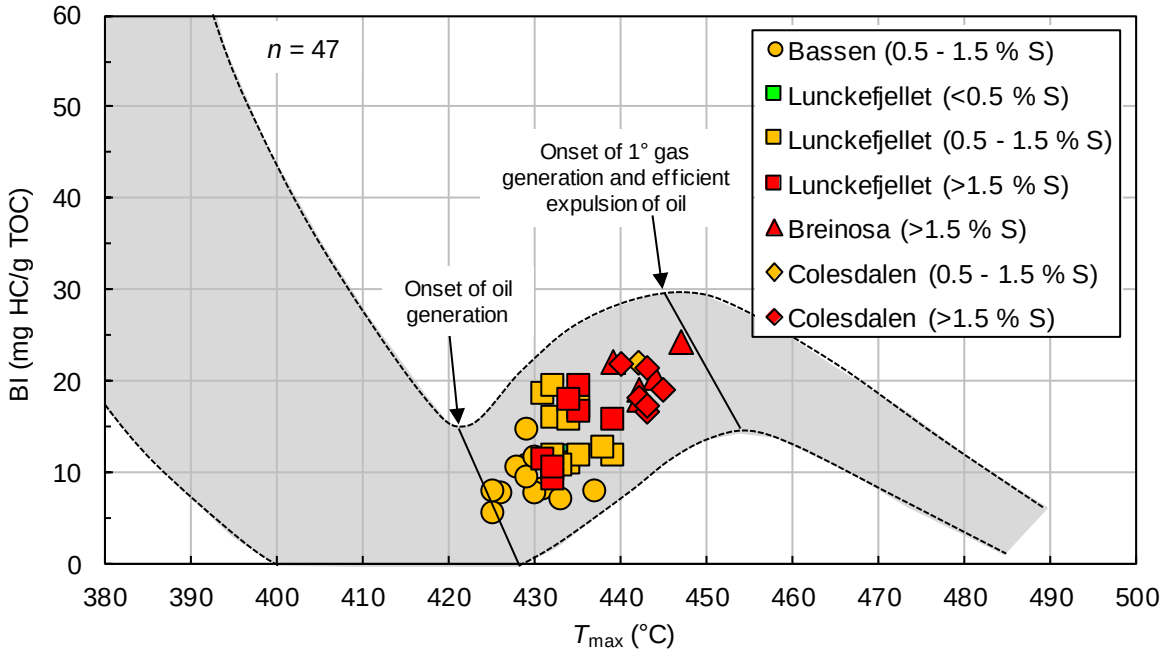

939

940

941 **Fig. 10c**

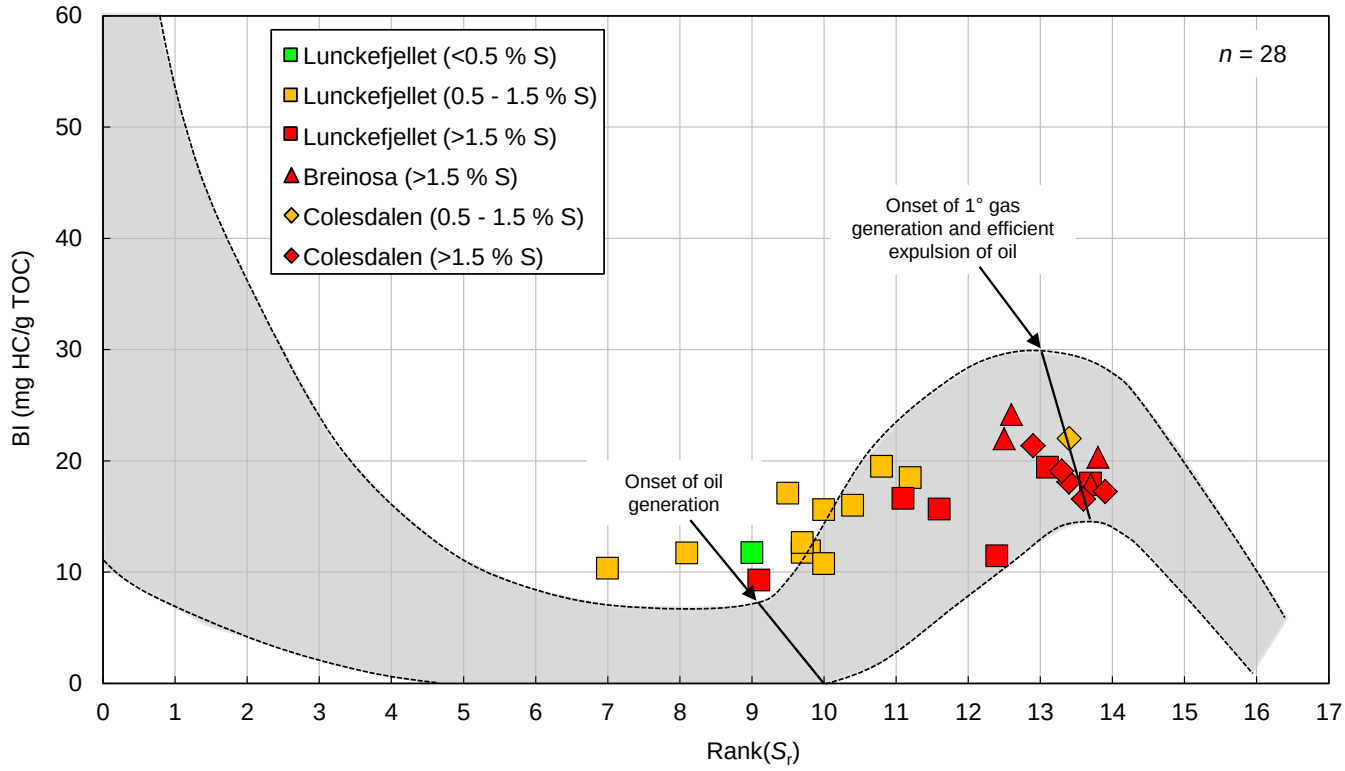

942

943

944 **Fig. 11**

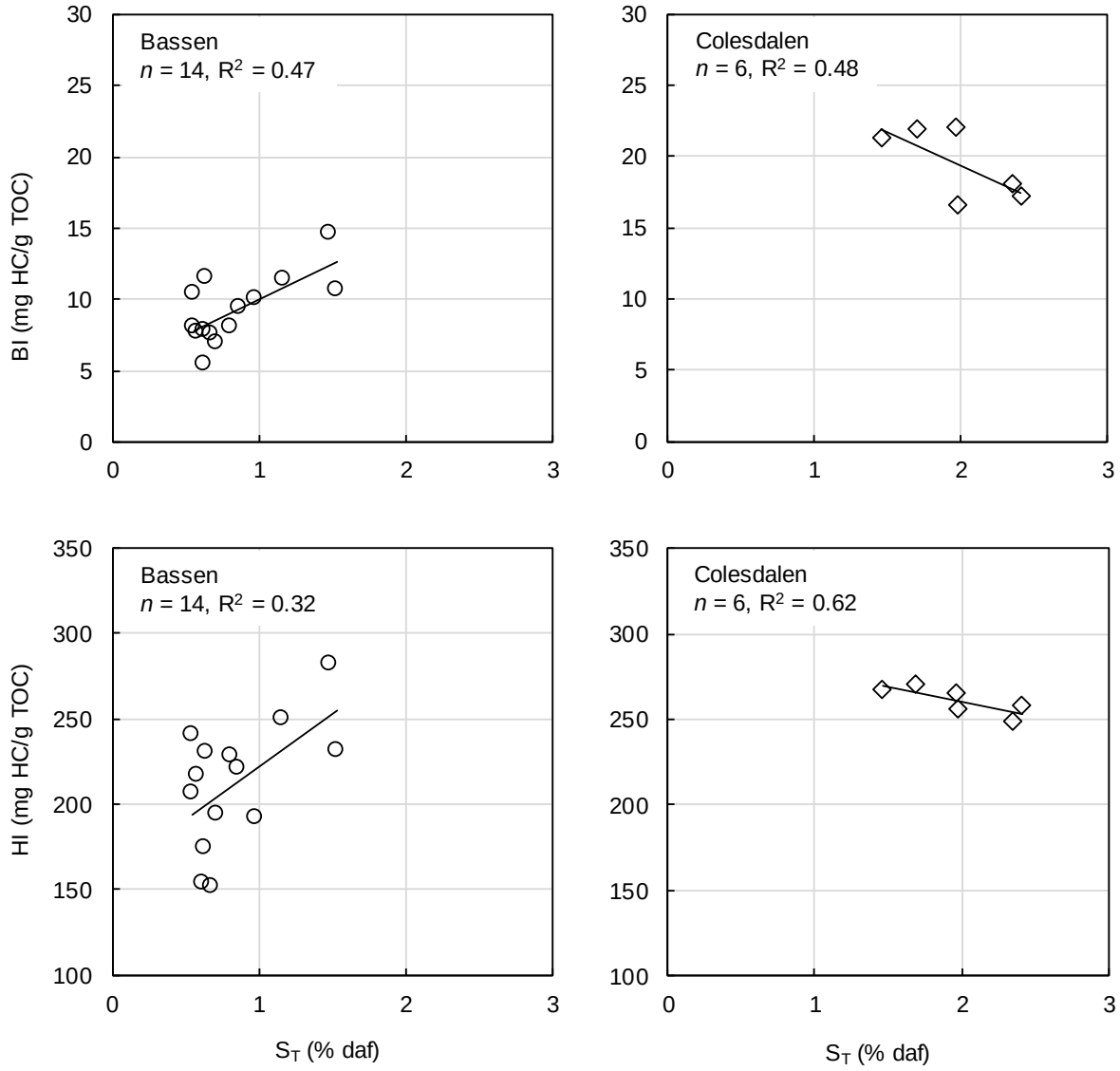

945

946 **Fig. 12**

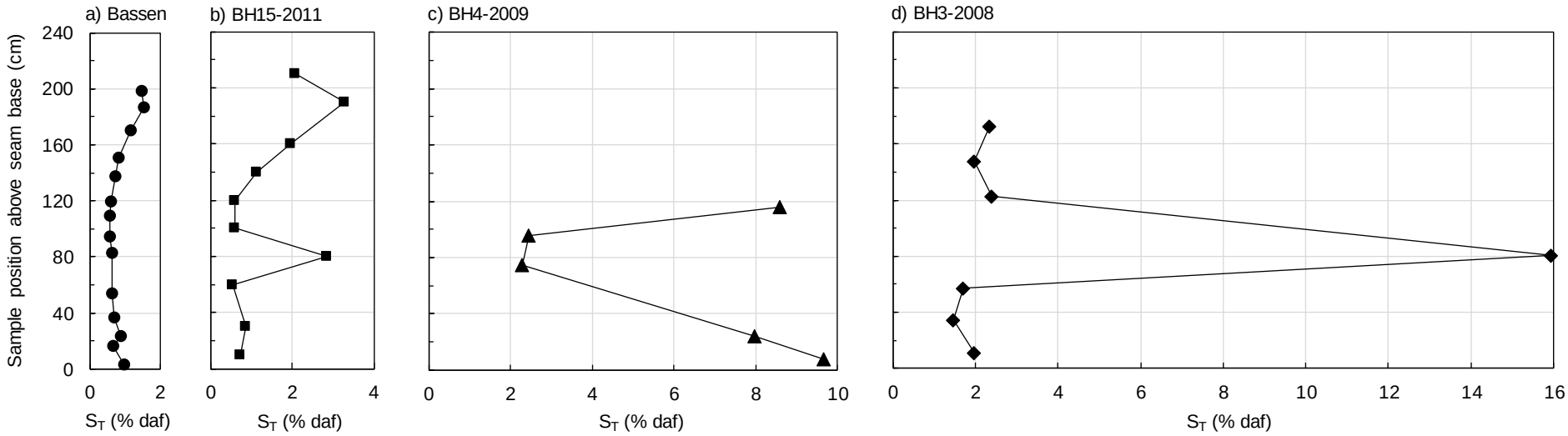

947

948 **Fig. 13**

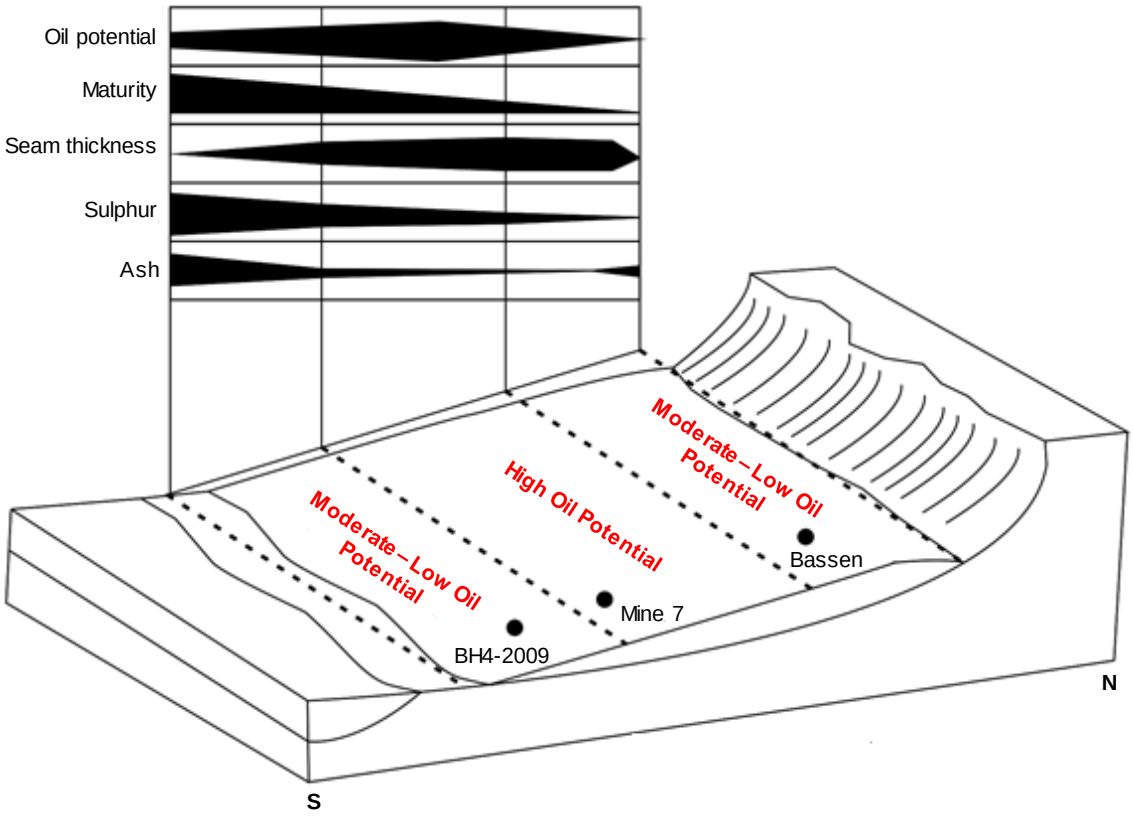

949